

# THE AERODYNAMIC DESIGN OF SECTION SHAPES FOR SWEPT WINGS

By H. H. PEARCEY

Aerodynamics Division, National Physical Laboratory,  
Teddington, United Kingdom

## 1. *Introduction*

KÜCHEMANN<sup>(1)</sup> has shown that the yawed wing and the swept wing-fuselage combination emerge as two of the acceptable solutions from the rationalization of the aerodynamic design of load-carrying and range-covering high-speed aircraft, provided the flow on the wing can be made analogous to that on an infinite yawed wing. This by definition implies similar velocity distributions at all points along the span with the isobars following the geometric lines of the sweep. The wing then has a two-dimensional equivalent with section and stream velocity identical to those normal to the leading edge of the analogous infinite yawed wing. The aerodynamic design of the sections can conveniently be studied on this two-dimensional equivalent, i.e. on an unswept model in a subsonic stream. Lock and Rogers<sup>(2)</sup> have shown that the section shape is naturally one of the starting points in a design method for achieving the ideal flow on finite swept wings. Research on the aerodynamic design of the section is thus complementary to that on the three-dimensional design features. In particular, it should be aimed at the derivation of chordwise distributions of thickness and loading which in combination will produce a favourable chordwise distribution of velocity and at the same time meet the structural and lifting requirements.

It was in this context that a fresh impetus was recently given to two-dimensional aerofoil research at the NPL. In presenting here a brief account of our attempts to evolve a systematic method of section design and improved shapes, the author is pleased to acknowledge that they formed part of a concerted research effort and as such benefited greatly from the experience and resources of the Royal Aircraft Establishment and interested members of the British aircraft industry. The author, of course, accepts full responsibility for the presentation and conclusions. Although the objective of the above mentioned efforts was the design of aircraft to cruise at a low supersonic speed, we have striven to keep

the research on section design sufficiently basic to be applicable for a wide range of sweep angles and hence a wide range of forward speeds corresponding to Mach numbers from around 0.7 to around 2.0.

## 2. The Aerodynamic Design Requirements

The whole essence of the cruising aerodynamic design of the type of wing under consideration is of course that it should be free from shock-wave drag. To be conservative, therefore, the cruise conditions will lie

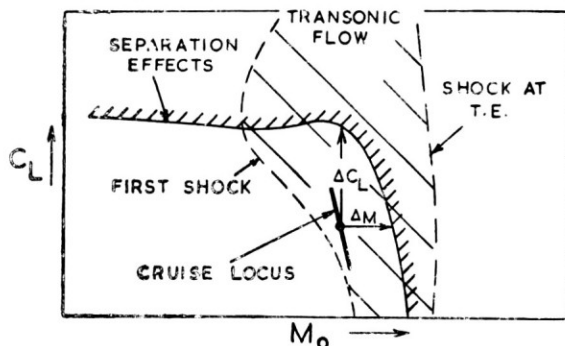


FIG. 1. Typical flow regimes near the cruise.

to the left (Fig. 1) of the line for the first appearance of shock waves on the wings i.e. to the left of the regime of transonic-type flow in which there is a shock wave somewhere between the leading and trailing edges. In practice, however, the transonic drag rise can usually be deferred beyond this stage.

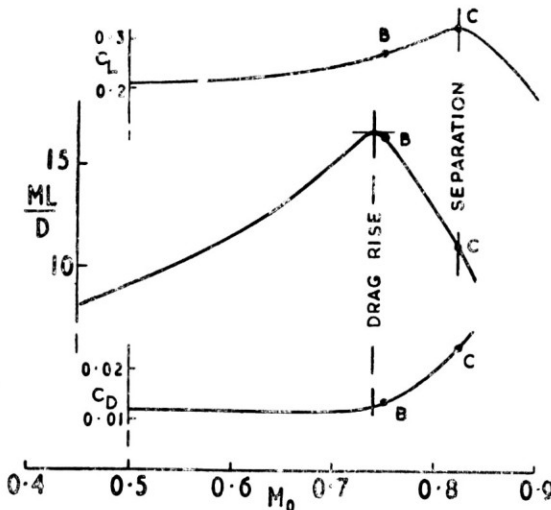


FIG. 2. Experimental results for typical aerofoil at fixed incidence (NACA 0009 $_{1/2}$  at  $2^\circ$ ; see FIG. 3).

with the range parameter,  $ML/D$ , increasing to a maximum value at some higher Mach number (Fig. 2). The most profitable cruising conditions lie at this maximum, or at a point just beyond for which the value has fallen by some small percentage of the maximum depending on which

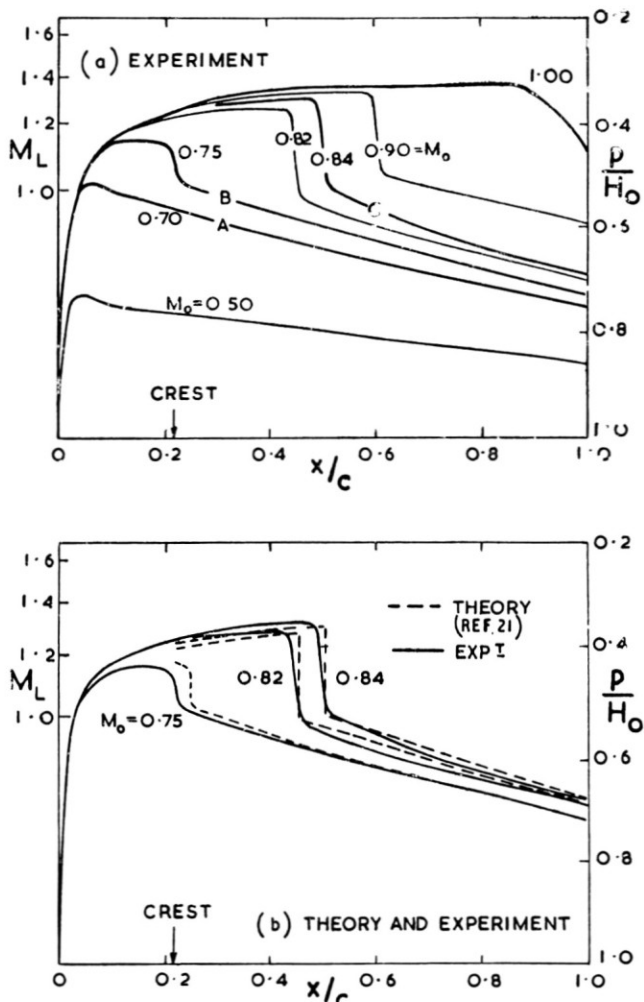


FIG. 3. Typical development of pressure distribution on the upper surface of an aerofoil (NACA 0009 $\frac{1}{2}$  at  $2^\circ$ ).

particular variation of the costing formula is used for a particular application. The cruise locus will therefore lie inside the transonic regime, with a region of local supersonic flow and probably a weak shock wave already formed on the upper surface of the wing (Fig. 1). The pressure distribution will be like that of curve B in Fig. 3(a), rather than that of

curve A which applies throughout the subsonic regime up to this condition. A good section for the cruise condition is thus one that helps to retard the development of local supersonic flow and the growth of shock strength to the stage at which it produces significant drag.

However, there are other important features of the flow development that are strongly influenced by the section shape and therefore that have to be taken into account in designing the section.

Firstly, the feasibility of cruising on the optimum cruise locus will depend on there being adequate margins of Mach number and lift coefficient before the strength of the shock wave that has already formed has increased still further to the stage at which it provokes severe boundary-layer separation (e.g. curve C of Fig. 3(a))\* . These margins are required to allow manoeuvres, gust encounters and other inadvertent change of flight conditions to remain free from buffeting and other undesirable separation-induced phenomena.

(It has often been suggested that the initial transonic drag rise is in fact associated with shock-induced separation, but this will not be so for the properly treated wing under consideration—not at full scale, nor at model scale provided either that the boundary layer is turbulent at the shock wave or the Reynolds number is reasonably high. In all such cases the shock will have generated a substantial increase in drag before it has become strong enough to provoke serious separation effects<sup>(4)</sup>. Exceptions to this may arise on swept wings for which the three-dimensional design is not fully successful, with local separations occurring early on some parts of the span to cause the flow to diverge even further from the pattern with fully swept isobars and thus indirectly to contribute to the wave drag. Extraneous form drag sometimes also occurs, near or even before the conditions for the wave-drag rise, if the adverse pressure gradient at the rear of the upper surface is so strong and/or the turbulent layer is so thick that a rear separation occurs<sup>(7)</sup>.)

Secondly, of course, airfield performance of the aircraft will depend on the lift coefficient that can be carried on the wing without trouble from low speed boundary-layer separation.

Naturally, one strives to make a design for good cruising performance compatible with that for delaying separation, at both high speeds and low speeds, but this is not always possible and we shall see that some of the ways of improving cruising performance by section design are definitely incompatible, either with the requirement for adequate buffet-

\* The development of the pressure distribution shown in Fig. 3 is that for increasing  $M_0$  at fixed incidence. An exactly similar build up in shock strength occurs for an increase in lift at fixed  $M_0$ <sup>(8)</sup>.

free margins above the cruise or with the requirements on airfield performance<sup>(3, 5)</sup>. This does not rule them out of consideration, however, because the separation effects can be postponed by boundary-layer control, for high speeds as well as for low speeds if necessary<sup>(5)</sup>, with the boundary-layer control device as an essential feature of the design to permit the maximum advantage to be taken of the shapes that are best for postponing the drag-rise Mach number.

### 3. A Basis for Rational Design and Research

*3.1 The need to predict shock-wave behaviour empirically*—The problems outlined above have of course been well known for many years. The main reason for the prolonged absence of anything like a general solution has been the inability to predict the development of the mixed subsonic/supersonic flows and the behaviour of the shock waves that they contain, and hence the inability to predict for a given section shape the conditions for the onset of the drag rise and the separation that these shock waves provoke. The purely mathematical solution for pressure distributions with shock waves has remained intractable in spite of the elegant work in the 1950's of mathematicians in many countries. We thus considered it necessary to establish an empirical method which, for reasons to be outlined below, would be capable of generalization to non-lifting and lifting aerofoils for a very wide range of conditions. The value of such a method has in fact already been proved in the research in progress and in applications to certain aircraft projects.

*3.2 The transformation from three dimensions to two*—In the same way as we were able to outline the aerodynamic problems on a single Mach number scale in Fig. 1, to be stretched according to the sweep angle,  $\phi$ , by

$$M_{3D} = M_{2D} \sec \phi \quad (1)$$

so the study of section effects appropriate to a wide range of forward speeds and sweepback can be confined to a very narrow band of high subsonic speeds in two dimensions. However, the factors on lift coefficient and thickness/chord ratio, namely,

$$(C_L)_{3D} \sec^2 \phi = (C_L)_{2D} \quad (2)$$

$$(t/c)_{3D} \sec \phi = (t/c)_{2D} \quad (3)$$

are such that the stretching is now in the ranges of values of these variables that have to be covered in the two-dimensional studies.

*3.3 The interplay between the design variables for the swept wing*—The interplay between Mach number, lift coefficient, thickness and sweepback for any particular aircraft design is such that a knowledge of the section

characteristics is a prerequisite for the choice of a desirable combination of these variables. This interplay was shown very clearly by Bagley<sup>(6)</sup> in a broad review of the section design for a transport aircraft. He first assumed that the cruising Mach number (in his case 1.2) would coincide with the first attainment of local supersonic flow normal to the isobars on the upper surface of a fully treated wing, or rather on its infinite yawed-wing equivalent. He then proceeded to estimate from an approximation to existing subsonic theory<sup>(8)</sup> what values of lift coefficient could be carried

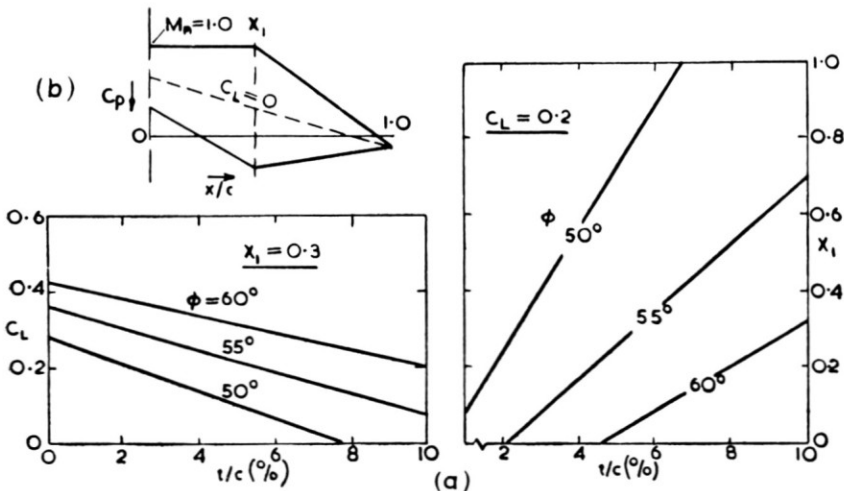


FIG. 4. Interplay between design variables for  $M_1 = 1.2$  cruise (Ref. 6).

on wings of various thickness and sweepback and for various types of assumed velocity distribution on the upper surface. Thus, any point on one of the curves in Figs. 4(a) (or on an interpolated curve) represents a combination of design conditions that would produce at  $M_0 = 1.2$  an upper-surface velocity distribution of the roof-top form shown in the inset diagram, with the plateau velocity just sonic. Any such combination gives the desired wing flow for the cruise, and the designer's task remains to choose the one that he can best reconcile with other requirements.

**3.4 The importance of the upper-surface velocity distribution** — Bagley's work pointed to just the type of generalization that is needed, and that is indeed possible in terms of the low-speed, upper-surface velocity distribution within the limitations of his simplifying assumptions. For the results of Fig. 4(a), one particular thickness form was assumed to apply throughout, and the camber line was varied (according to thin aerofoil theory) to maintain the same upper surface velocity distribution. If desired, the thickness form could also be varied, with the camber line again adjusted

to maintain the specified upper-surface velocity distribution\*. In this way it might be possible to increase the lift coefficient at the cruise conditions—by carrying more load towards the trailing edge, for example—or to optimize in some other manner. Variations can also be made, of course, in the initial choice of upper-surface velocity distribution, e.g. in the extent of the plateau in the roof-top distribution (Fig. 4(b)). Bagley<sup>(6)</sup> considered other variations, including the change to a linearly decreasing velocity from leading edge to trailing edge, the effect of allowing the velocity to become locally supersonic on the upper surface, the effect of carrying increased load at the trailing edge on the same thickness form etc.

This type of calculation can show trends only, however, and leaves open such important questions as: Just how much can the velocity be allowed to exceed sonic locally without incurring strong, drag-producing shock waves, and how does this in turn depend on the form of the velocity distribution and section shape? How far can the flat top be pushed without increasing too strongly the adverse pressure gradient at the rear and how are the various combinations represented by the drag-rise lines reconcilable with shock-induced separation onset?

Now it is immediately obvious that very great advantages would accrue if the necessary extension to this analysis, namely, a method for predicting pressure distributions with shock waves, could be based in some way on the subsonic distribution. In particular continued use could be made of the type of analysis just described and of the powerful methods that exist for designing aerofoils to produce prescribed subsonic velocity distributions<sup>(8, 10)</sup>.

The low-speed velocity distribution holds its form at least up to the stage at which sonic velocity is exceeded locally on the upper surface. The familiar pressure distribution of the type shown in Fig. 3(a) indicates that the change from this subsonic distribution to the distribution appropriate for  $M_0 = 1.0$  (the sonic-range distribution) is a progressive transformation, with intermediate distribution related part to one and part to the other, and with the shock-wave pressure rise joining these two parts. This suggests that the desired method of predicting shock behaviour, and hence of design, might well be established from these two basic pressure distributions—the subsonic and the sonic-range.

The results reproduced in Fig. 5 provide a clear demonstration of the usefulness of this concept. The two aerofoils<sup>†</sup> of different thickness/chord

\* The analytically defined, infinite family of thickness distributions described by Tanner<sup>(9)</sup> is extremely useful in this respect.

† For convenience, various section shapes will be referred to by numbers allocated to them in the current series of tests at the NPL. Details will be issued in due course.

ratio (12% and 8%) were designed to have as nearly as possible identical subsonic and sonic-range velocity distributions on the upper surface.\*

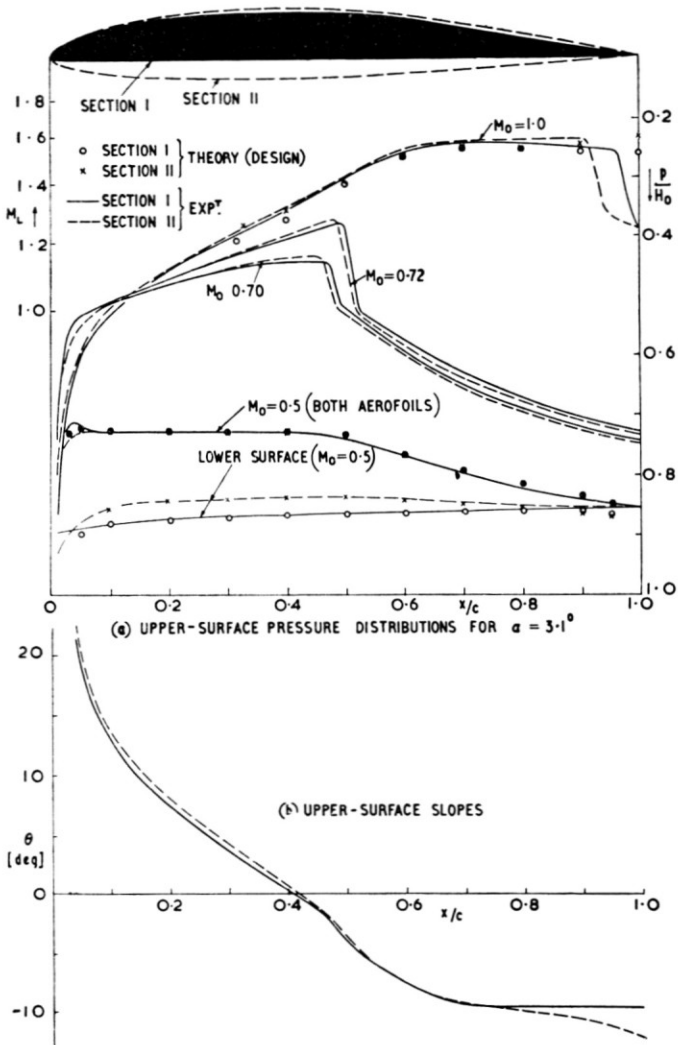


FIG. 5. Comparison of design and results for two aerofoils with the same upper-surface shape and flow. (See also FIG. 5(c).)

They exhibited to a remarkable degree the same development of the local supersonic regions and shock waves (Fig. 5(a)) as Mach number was

\* The method of design for a given sonic-range velocity distribution and the importance of the surface-slope distribution (Fig. 5(b)) will become obvious later.

increased, at the appropriate design incidence in each case.\* As a consequence of this, the Mach numbers for drag rise and separation onset were identical (Fig. 5(c)). The corresponding values of lift coefficient were, of course, different because different camber lines were needed

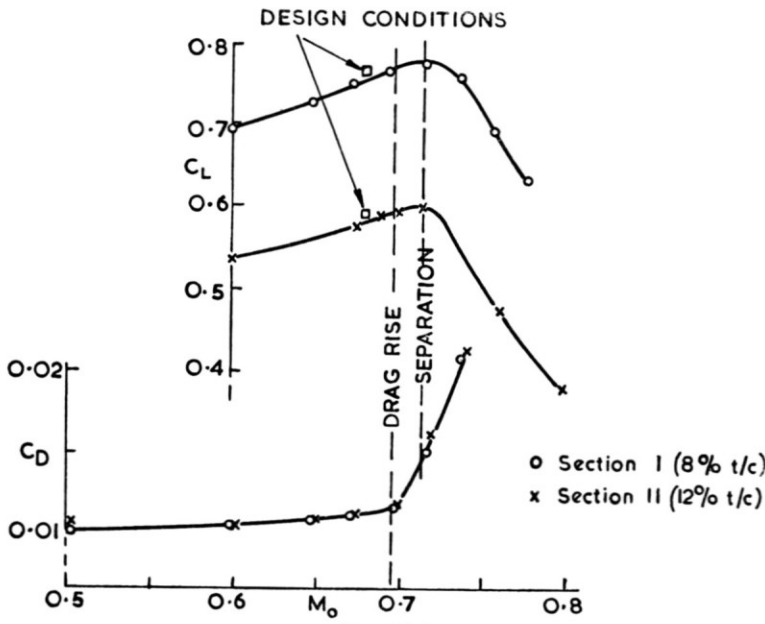


FIG. 5(c).

to reconcile the different thicknesses with the same upper-surface pressure distribution; the difference in  $C_L$  (0.17) represents the exchange for the difference in thickness. It is also of interest that the margin of separation-free lift coefficient above the drag-rise condition was the same in both cases.

\* In devising a series of sections for research, it is convenient to specify "design" conditions that will serve as a criterion in assessing their relative merits, and important to reproduce these conditions systematically in experiments. In the NPL work we take special care to reproduce the design subsonic pressure distribution by finding for each model an equivalent incidence that is greater than the theoretical value by just the amount needed to offset the combined effects of boundary-layer growth and tunnel interference<sup>(11)</sup>. The design pressure distribution is found theoretically for  $M_0=0$  and factored appropriately (see Section 4.2) to  $M_0=0.5$ . The design  $M_0$  is then taken as that for which  $M=1.0$  locally at the crest when the distribution is stepped up beyond  $M_0=0.5$  by the chosen factor. (The crest is the point at which the tangent to the surface is parallel to the stream direction.) The design  $C_L$  is taken to be the value that would be reached at this design  $M_0$  for a Prandtl-Glauert increase from the observed  $C_L$  at  $M_0=0.5$ . The geometrical incidence is used in the derivation of a sonic-range pressure distribution to compare with experiment.

#### 4. A Method of Predicting Pressure Distributions with Shock Waves

4.1 *The component parts of the distribution*—On the strength of the results described in preceding sections, we can consider the flow on each surface separately once the circulation has been established by subsonic aerofoil theory. In the present context, in which we are concerned with strongly lifting aerofoils and only limited penetration of the transonic flow regime, we can confine our detailed attention to the upper surface. For this, we have to consider the basic subsonic and sonic-range distributions, and then the derivation from them of the three component parts of intermediate distributions, namely, the upstream supersonic flow, the downstream subsonic flow, and the shock wave accommodated between them in some compatible manner.

4.2 *The subsonic distribution*—Of the reliable approximate methods available<sup>(8, 10)</sup> for calculating the incompressible velocity distribution, that due to Weber is the most frequently used because of its adaptability to design and computation. Several compressibility factors are available for stepping this up to the correct free-stream Mach number with varying degrees of accuracy and validity to particular circumstances. The Prandtl-Glauert factor is the simplest to use, and also happens to give good agreement with our particular experimental results<sup>(12)</sup>. The most accurate for free-air conditions is probably that due to Woods<sup>(13)</sup>.

4.3 *The sonic-range distribution*—Of the several approximate methods that have been proposed, that due to Sinnott<sup>(14)</sup> is strongly preferred because of its greater reliability and range of applicability to lifting aerofoils. It takes properly into account the effect of both families of characteristics in the finite region of supersonic flow, and particularly the fact that the simple-wave expansion  $\omega_1(x)\{ = f(\theta)\}$  (see Fig. 7), is reduced by a compression  $\omega_2(x)$  to give the actual variation of Prandtl-Meyer angle,  $\omega(x)$ , or local Mach number  $M_L$ . The value of  $\omega$  is first found for the trailing edge point,  $\omega(T.E.)$ , in terms of the flow deflection from the surface on to the dividing streamline (assumed zero downwash)<sup>(15)</sup>, and then for the crest point,  $\omega(CR)$ , from an empirical relation in terms of a parameter  $\chi$  of leading-edge geometry (Fig. 7).  $\omega'_2(T.E.)$ , the total compressive effect reaching the surface between crest and trailing edge, is found from

$$\begin{aligned}\omega'_2(T.E.) &= \omega(CR) + \omega'_1(T.E.) - \omega(T.E.) \\ \omega'_1(T.E.) &= f(\theta) = f(\delta_{T.E.})\end{aligned}$$

The chordwise distribution of this compressive effect is assumed to be the same as in the theoretical solution for a double-wedge aerofoil.

In the recent work on cambered aerofoils, the method has been found to give reasonably good results, provided the ordinate  $Z$  in the parameter

$\chi$  is defined from the centre line (i.e. thickness only)\*. The agreement with experiment has not, however, reached the high standard achieved on the symmetrical aerofoils for which the method was produced originally,

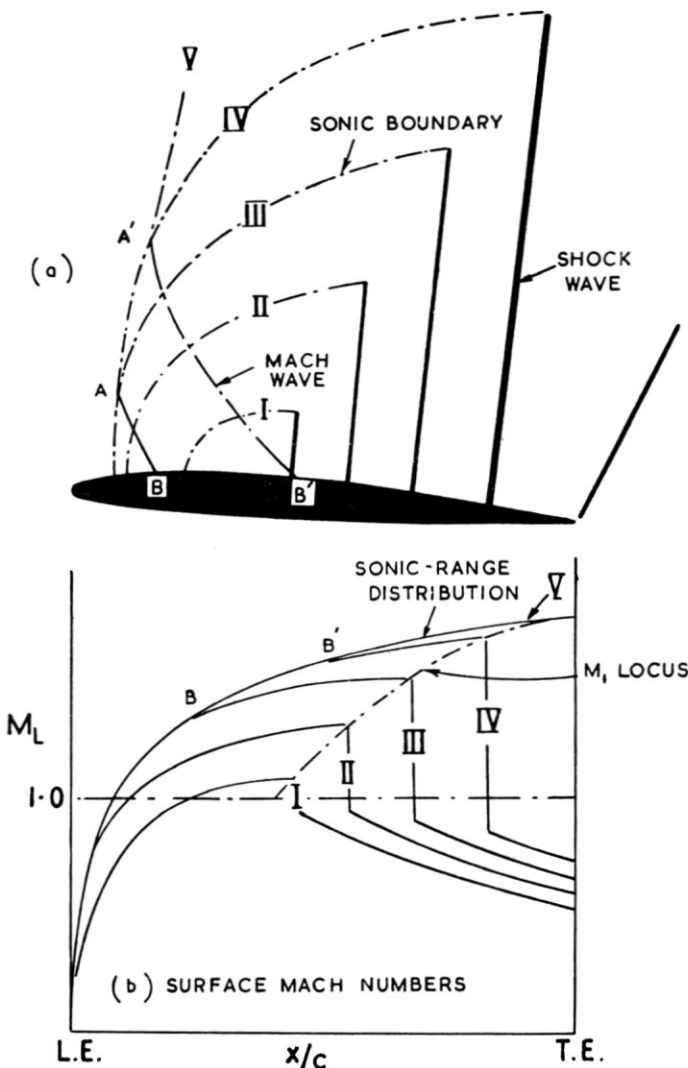


FIG. 6. The development of the region of local supersonic flow with increasing Mach number at fixed low incidence.

and we hope to improve the empirical derivation of  $\omega(CR)$  for cambered aerofoils as more results become available from the current research.

\* This differs from the definition used in calculations made by Sinnott<sup>(16)</sup> in anticipation that the ordinate from the chord line would be appropriate.

Randall<sup>(17)</sup> suggested a method for deriving the pressures upstream of the crest that are not given by Sinnott's method.

**4.4 The supersonic flow upstream of the shock**—For a given Mach number,  $M_0$ ,  $M_0^* < M_0 < 1.0$ , Sinnott finds the pressure at the crest,  $p_{CR}(M_0)$ , from an empirical relation between the pressure difference  $p(M_0) - p(1.0)$

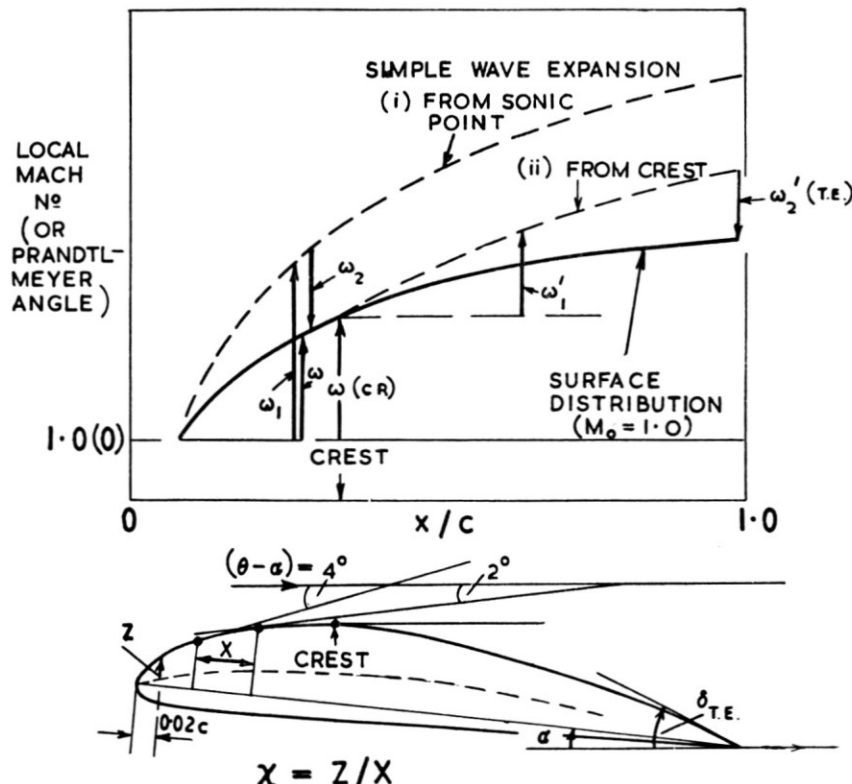


FIG. 7. Derivation of sonic-range pressure distribution and definition of empirical parameters.

$\{ = a \text{ in Fig. 8(a)} \}$  and the Mach number difference ratio  $(M_0 - M_0^*)/(1 - M_0^*)$ . This gives the point  $Q$  on the distribution in Fig 8(a). Once the shock position is known, the pressure  $p_1 M_0$  immediately upstream of the shock can be found from a similar empirical relation. The shock position is not known at this stage, however, and in order to proceed, a locus of possible values of  $p_1(M_0)$  is found for a range of chordwise positions. This gives the locus for  $R$ . When  $R$  is finally fixed, the distribution of the pressure difference  $a(x)$ , and hence of the distribution of surface pressure, can be found from a linear interpolation, in terms of distance, between  $a(R)$  and  $a(Q)$ .

4.5 *The subsonic flow downstream*—The pressure  $p(M_0)$  is found simply by applying a compressibility correction factor (e.g. Prandtl-Glauert) to the pressure at corresponding points in some low speed distribution.

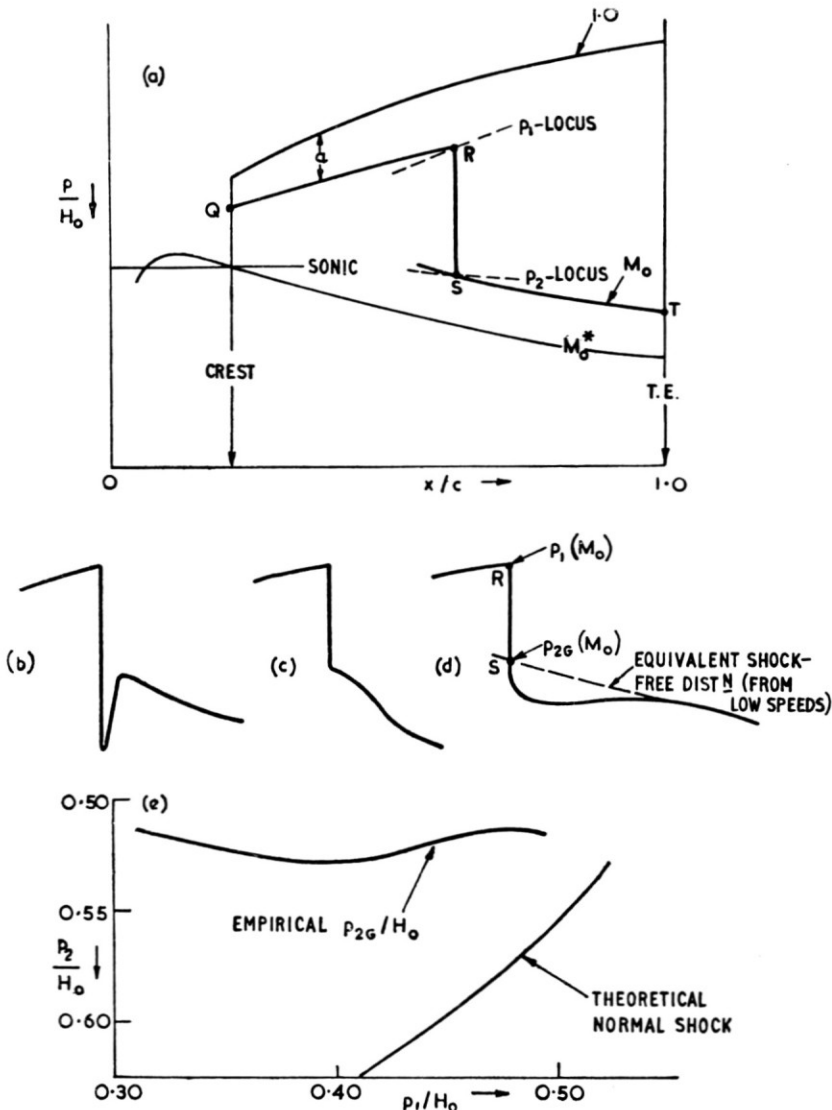


FIG. 8. Derivation of pressure distribution with shock wave.

This procedure gives good agreement with experiment, for points from the trailing edge,  $T$ , forwards towards the shock, for as long as the effects of any separation that may be present are confined to the immediate vicinity of the shock. At this stage in the derivation of the pressure distri-

bution, sufficient of the downstream part is drawn to pass through the anticipated shock position,  $S$ .

*4.6 The shock itself*—The position of the shock will be determined by finding the point at which the pressure rise from the supersonic flow to the subsonic flow is just appropriate for an aerofoil shock with the local value of upstream Mach number, or upstream pressure,  $p_1$ . This is done by drawing a locus of shock downstream pressures,  $p_2(M_0)$ , to correspond to that of  $p_1(M_0)$  using the appropriate function,  $p_2 = f(p_1)$ . The determination of this function proved to be the key to the whole derivation. Two main reasons contribute to its difference from the function for normal shocks in uniform, inviscid flow. Firstly, as pointed out originally by Ackeret, Feldmann, and Rott in 1946<sup>(18)</sup> and examined analytically by Emmons<sup>(19)</sup> and others, the non-uniformity of the shock and the curvature of the surface require a readjustment of the transverse pressure gradient which results in a rapid chordwise expansion immediately following the shock, Fig. 8(b). Secondly, the interaction with the boundary layer at its foot produces a sudden increase in displacement thickness which Gadd and Holder<sup>(20)</sup> have shown to apply even for uniform upstream flow, Fig. 8(c). In a finite region of supersonic flow on a curved surface, both effects combine to give the form of variation shown in Fig. 8(d). To overcome the uncertainties, and the dependency of the effective shock pressure-rise on aerofoil curvature, boundary-layer thickness, etc., Sinnott and Osborne<sup>(21)</sup> defined an equivalent shock pressure-rise  $p_{2G}(M_0) - p_1(M_0)$  where  $p_{2G}(M_0)$  is the pressure that would apply at the shock position if the downstream subsonic distribution (determined as above using the Prandtl-Glauert factor) were extrapolated forward to meet the shock at  $S$  (in Fig. 8(d)). They analysed experimental results on this basis to produce the simple empirical relation shown in Fig. 8(e), with only a small amount of scatter. This relationship can now be used for the derivation of the  $p_2$  locus in Fig. 8(a). The intersection of this locus with the downstream pressure distribution gives the point  $S$  in Fig. 8(a), hence the shock position, and finally admits the completion of the upper-surface pressure distribution from the crest to the trailing edge.

*4.7 The lower-surface distribution*—If this is needed, to complete the calculation of lift say, it can be found by factoring the appropriate low-speed distribution by the favoured compressibility factor right through to the stage at which the shock-induced separation on the upper surface disturbs the trailing edge pressure and hence the circulation<sup>(22)</sup>, provided the velocities thus determined do not exceed the sonic value, in which case the lower surface would be treated separately as described above for the upper surface.

**4.8 Comparison with experiment**—The agreement is good (Fig. 3(b)) up to the stage at which the effects of shock-induced separation spread to the trailing edge (curve C of Fig. 3(a)) and so destroy the basis of the method by disturbing the downstream pressure distribution and the definition of the equivalent pressure rise. Small discrepancies in pressure often occur locally downstream of the shock, due to the local effect described above. Discrepancies also occur in the upstream supersonic flow when the development of the flow departs too far from the pattern sketched in Fig. 6, for which the upstream sonic point is fixed and the pressures at fixed points tend to their values in the sonic-range distribution as limits. These discrepancies become most noticeable at high incidences, when there are substantial rearward movements of the sonic point as the stagnation point moves towards the leading edge from the lower surface with increase of  $M_0$  towards 1.0, but the practical consequences are not serious except for one particular type of section shape of interest to be described below. The reason for this is that the shock position, which is one of the most important features of the distribution, can nearly always be predicted quite accurately in spite of the other discrepancies. This in turn results from the fact that the equivalent downstream pressure, as defined, is so nearly constant that the position of the intersection of the  $p_2$  locus with the downstream pressure distribution is almost independent of  $p_1$ .

### 5. The Prediction of Section Characteristics

**5.1 The drag rise**—Although, as we shall discuss more fully later, the appearance of low pressure supersonic flow on the rearward facing areas

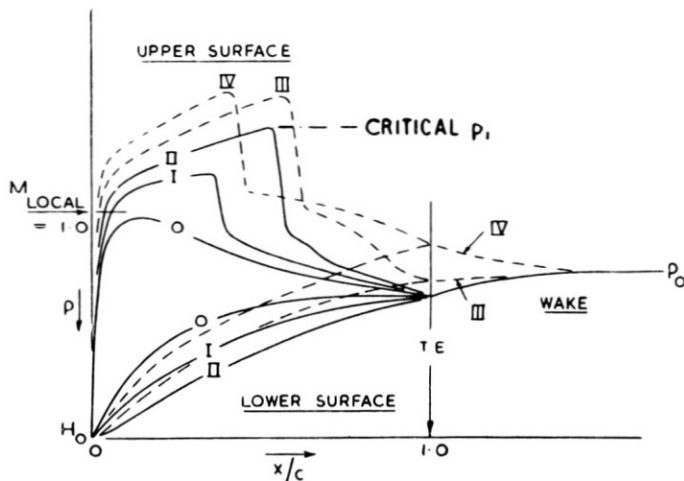


FIG. 9. Pressures for successive stages in an incidence increase at fixed Mach number.

of the wing behind the crest is neither a necessary nor a sufficient condition for the occurrence of wave drag, it has, following Nitzberg and Crandall<sup>(23)</sup>, often successfully been used as a criterion for the onset of the

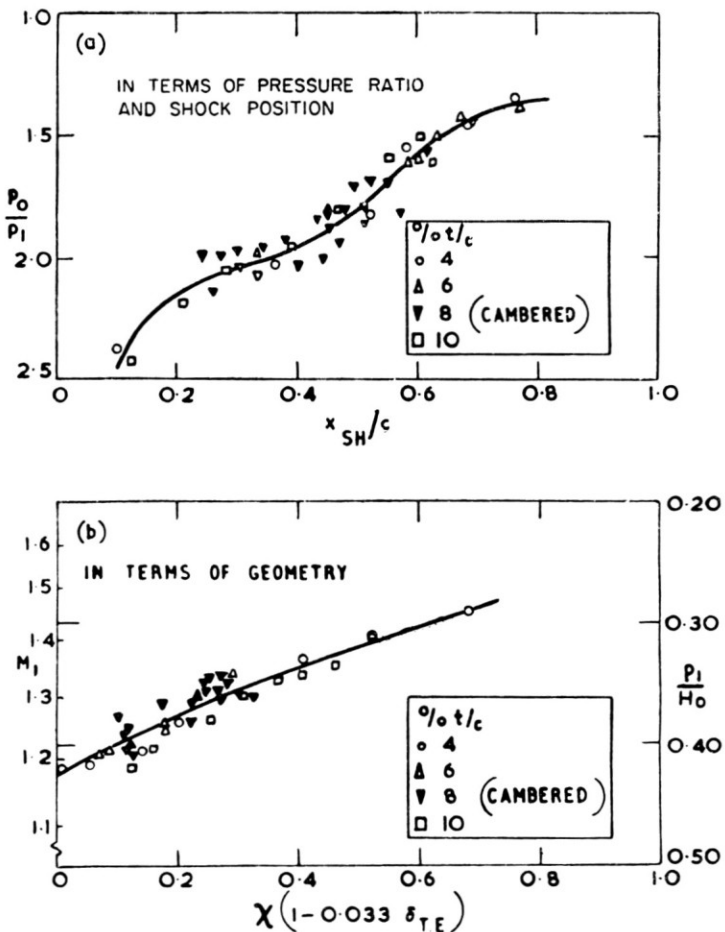


FIG. 10. Different correlations of critical values of  $p_1$  for trailing-edge pressure divergence.

transonic drag rise. Expressed in other words, this criterion states that the drag starts when the shock wave passes over, or first appears to the rear of the crest. On this basis, the drag rise can be predicted from the pressure distributions derived as above, and Sinnott<sup>(16)</sup> has shown that this approximates to finding when  $p_{CR}/H_0 = 0.515$  in the equivalent shock-free distribution, or alternatively when  $p_{min}/H_0 = 0.498$  for extensive roof-top pressure distributions with  $p_{CR}$  on the plateau. His prediction is

in fact accurate for the majority of section shapes. The exceptions and the consequent limitations of the method will be discussed below.

**5.2 The onset of separation effects**—Since we are here interested only in the onset of significant effects on the magnitude and steadiness of the loads on the aerofoil, we can use the divergence of trailing-edge pressure as a criterion<sup>(22)</sup>, i.e. stage III of Fig. 9, and so by-pass considerations of how the aerofoil shape affects the first occurrence of separation locally at the shock and its subsequent development to the stage at which it influences the trailing edge, both of which are related to the difficult question of what the actual shock pressure-rise is (see Fig. 8). It is found that the

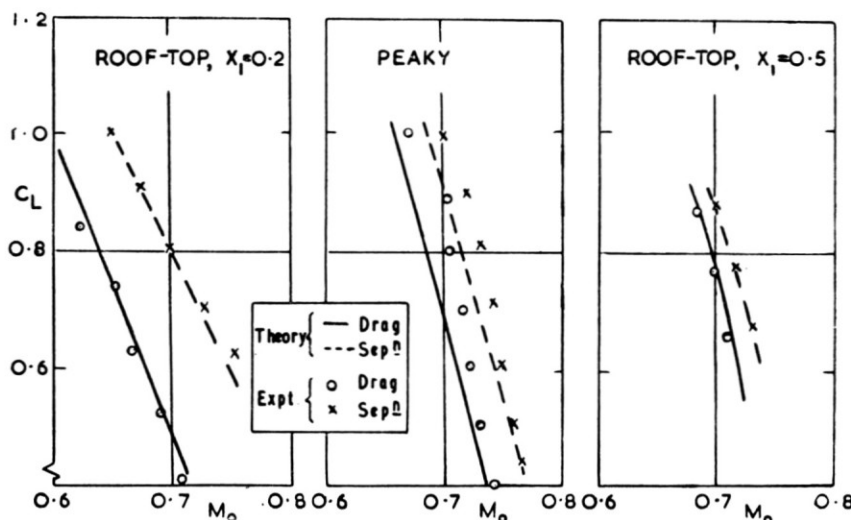


FIG. 11. Comparison between predicted (Ref. 21) and measured results.

particular value of shock upstream pressure,  $p_1$ , that is critical for trailing-edge pressure divergence varies appreciably with aerofoil geometry (Fig. 10(b)), or, alternatively, that its ratio to the pressure in the freestream varies appreciably with shock position (Fig. 10(a)). These correlations\* still show a fair amount of scatter, and it is hoped to produce an improved one by studying the reasons for the variations. In the meantime either correlation forms a reasonable basis for prediction, using a pressure distribution produced by Sinnott's method†.

\* The first (Fig. 10(b)) is a modification of the one used originally by Sinnott<sup>(16)</sup> (due to J. Osborne) and the second is a modification of one produced more recently by G. E. Gadd.

† The prediction will be conservative in the sense that the first divergence of trailing-edge pressure marks the onset or "threshold" of separation effects<sup>(22)</sup>; the effects are usually not serious until a later stage is reached.

5.3 *Comparison with experiment*—It is here convenient to predict the aerofoil pressure distributions from measured low-speed distributions, and the sonic range distributions from appropriate experimental incidences. Viscous effects on the circulation and the shock-free flow are then largely eliminated from the comparison. Some of the comparisons given by Sinnott<sup>(16)</sup> are reproduced in Fig. 11 to show that the agreement is remarkably good in many cases. The exception in Fig. 11(b) occurred for an aerofoil for which the development of the local supersonic flow was expected to be more favourable than predicted (see below). Table 1 shows comparison obtained more recently.

TABLE 1

| Section |       | Design            | Measured | Sinnott's prediction<br>(ref. 16) |
|---------|-------|-------------------|----------|-----------------------------------|
| 1       | $M_0$ | 0.68              | 0.70     | 0.70                              |
|         | $C_L$ | 0.765             | 0.77     | 0.79                              |
| 11      | $M_0$ | 0.68              | 0.70     | 0.70                              |
|         | $C_L$ | 0.59              | 0.59     | 0.61                              |
| 4       | $M_0$ | 0.67              | 0.70     | 0.68                              |
|         | $C_L$ | 0.87 <sub>1</sub> | 0.965    | 0.89                              |
| 2       | $M_0$ | 0.65              | 0.64     | 0.66                              |
|         | $C_L$ | 0.73              | 0.72     | 0.74                              |

5.4 *Prediction from theoretical information*—Sinnott<sup>(16)</sup> has shown that the prediction can be made entirely from theory, and suggests that the order of approximation used for such quantities as the compressibility correction factors and lift-curve slope can be adjusted according to whether accurate design data are required, or rapid qualitative comparisons between

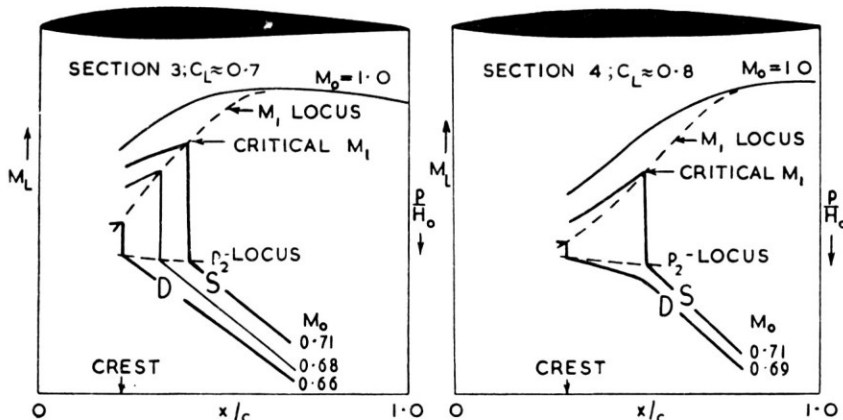


FIG. 12. Theoretical comparison between sections (Ref. 15).

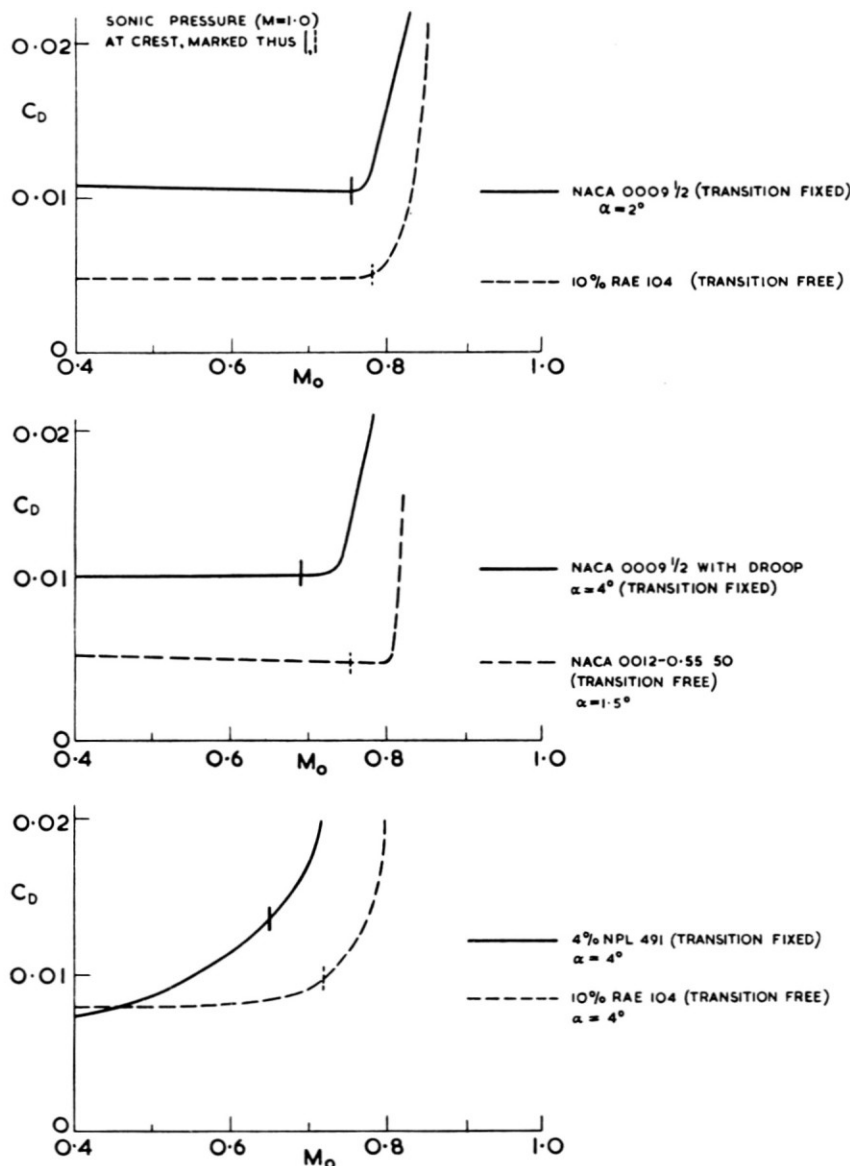


FIG. 13. Experimental results for miscellaneous sections.

section shapes for which some relaxation in absolute accuracy is admissible. Fig. 12 illustrates the value of such comparisons. Upper-surface pressure distributions were predicted on the assumption of inviscid flow and adherence to the Prandtl-Glauert compressibility factor. They demonstrate how, starting from different drag-rise Mach numbers (curves D), the critical shock upstream pressures,  $p_1$ , for separation onset (curves S)

are reached at the same value of  $M_0$  after quite different intervals, and that the reasons for this are the more rapid shock movement for aerofoil 3 than for aerofoil 4 and its higher value for critical  $p_1$ . These features are inherent in the design but only revealed by an analysis of this kind.

### 6. Further Discussion on the Factors Affecting the Wave Drag

The wave drag is transmitted to the surface by a readjustment in the pressure distribution, but the corresponding momentum losses occur at the shock itself. These losses, which at first are approximately proportional

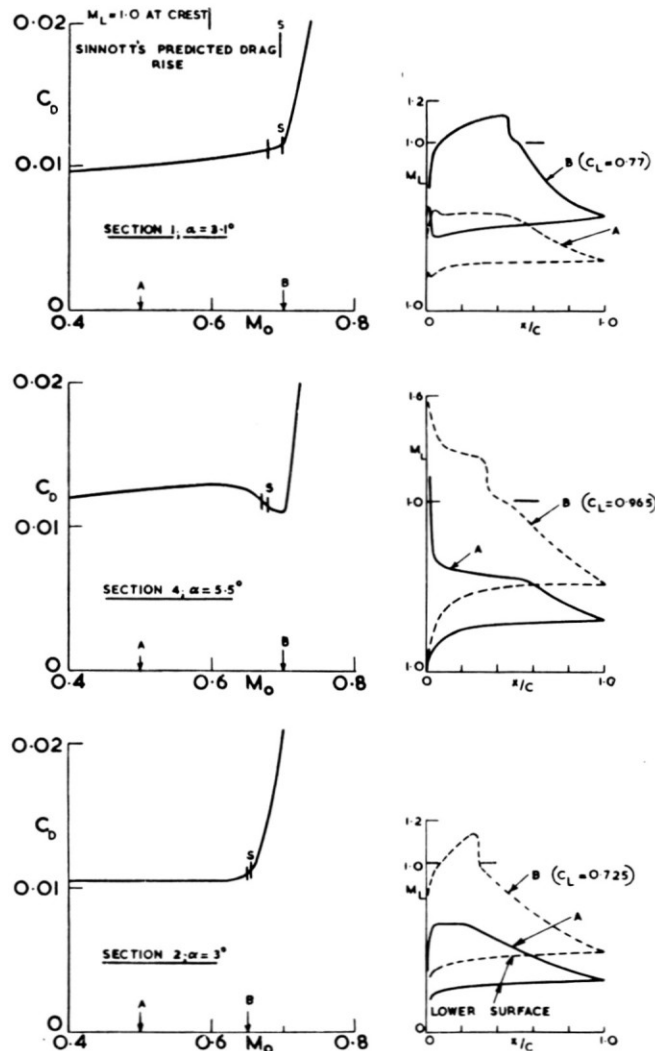


FIG. 14. Results from tests on 8% thick sections designed for specific types of upper-surface pressure distribution.

to  $(M_1^2 - 1)^3$ , build up only slowly as the upstream Mach number first increases from unity. Moreover, the appearance of a Mach number appreciably greater than unity is not necessarily indicative of a significant wave drag, because some isentropic compression ahead of the shock is possible and also because the losses at the shock can fall rapidly to zero above

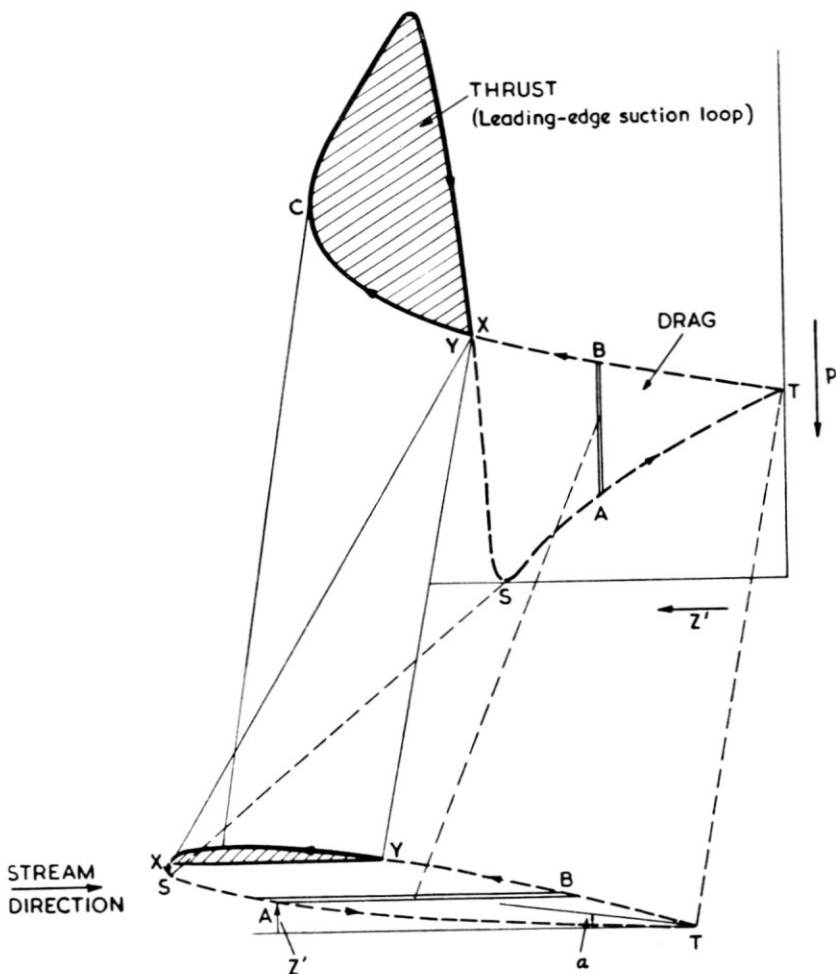


FIG. 15. Drag analysis of surface pressures.

the surface if the shock is short. We believe the real significance of the passage of the shock to the rear of the crest to be that for most aerofoils it coincides with a simultaneous increase in shock upstream Mach number and height as the stream tubes well above the surface are allowed to expand more freely. If the shock can be kept weak as it passes over the crest, then the drag rise can be delayed, and vice-versa, if the shock becomes unduly

strong or high before it crosses the crest, it can cause a premature drag rise.

Analysis of existing data (Fig. 13) revealed that the drag-rise behaviour could be classified broadly into three groups according to whether the rise

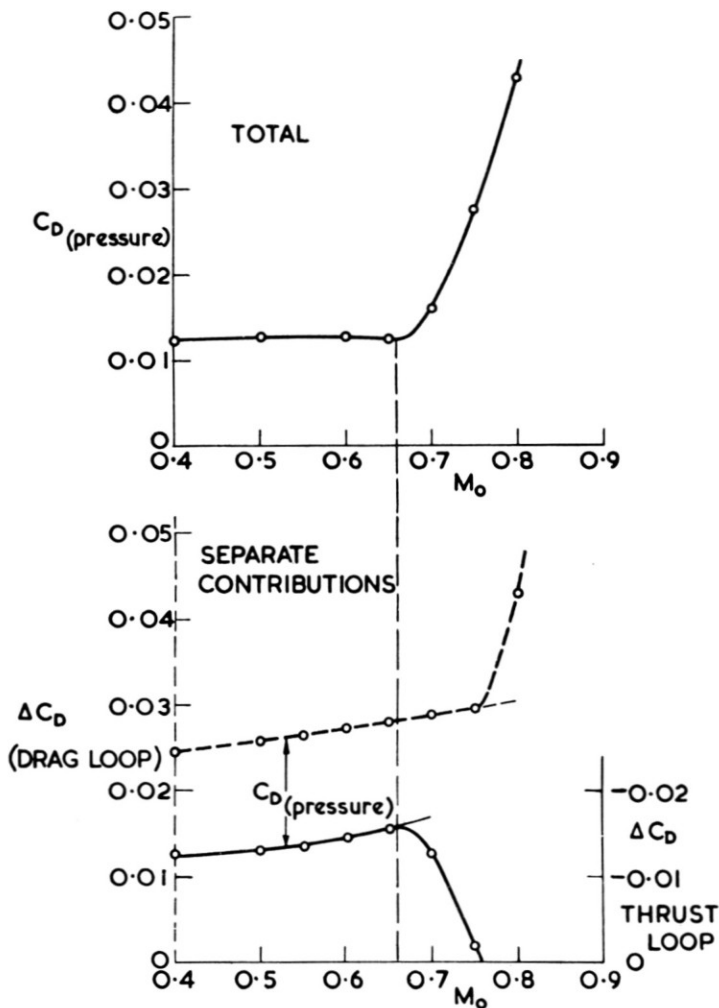


FIG. 16. Results for NACA 0009 $\frac{1}{2}$  at  $\alpha = 4^\circ$ .

coincided with the appearance of supersonic flow to the rear of the crest (indicated by the attainment of  $M = 1.0$  at the crest); followed it only after a measurable interval; or preceded it. The first group is the largest, the second holds promise of advantage in design, and the third of disadvantage.

In order to explore these differences in behaviour and to seek a correlation with types of section shape and low-speed pressure distribution,

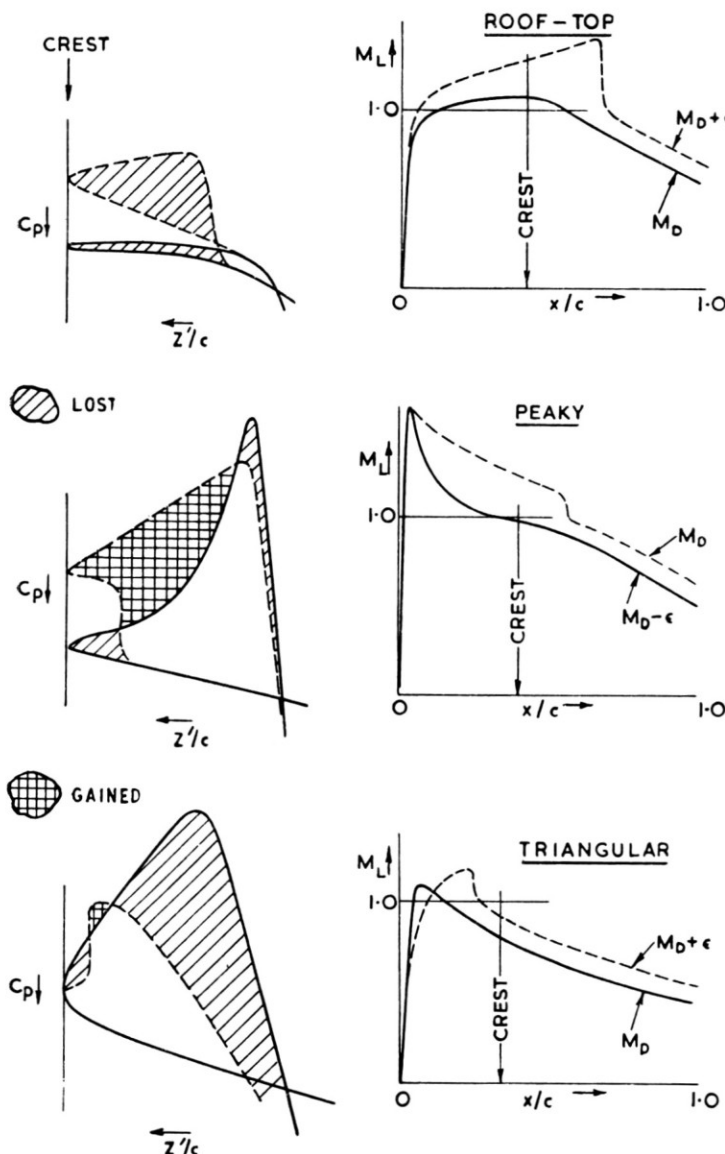


FIG. 17. Types of upper-surface pressure distribution and corresponding suction loops.

we found it convenient to plot the surface pressures in the manner shown in Fig. 15. Direct integration of the area gives the pressure drag. The curves usually divide into two main loops—a suction loop and a drag loop, approximately equal to one another, at first for each aerofoil and incidence, but differing in size and shape from case to case, i.e. from

aerofoil to aerofoil and from incidence to incidence. The initial changes in wave drag can be traced to a decrease in area of the suction loop (Fig. 16) and so we can focus attention to this loop. It is generated by a range of the upper surface on either side of the crest.

The three types of behaviour shown in Fig. 13 are characterized by the shape of the suction loop and of the upper-surface pressure distribution approximately as shown in Fig. 17. The roof-top distribution conforms to the  $M = 1$  at crest prediction of drag rise because the development to the rear of the crest folds the loop inside out, to convert it into a drag area. The distribution of local supersonic flow from the favourable peaky distribution leads to an increase in suction on forward facing areas between the peak and crest to add fullness to the loop there and so to offset losses elsewhere, even when the shock has passed to the rear of the crest; an isentropic compression from a relatively high supersonic Mach number at the peak to a lower one at the shock is implicit in this behaviour. The triangular distribution usually gives unfavourable results because the suctions on the right-hand side of the loop (and hence from very near the leading edge) decrease in proportion to the dynamic head, and the loop begins to collapse before the crest pressure is sonic.

Recent tests on aerofoils designed to reproduce these types of pressure distribution at prescribed conditions have confirmed this analysis (Fig. 14). We now realize that the design of section 4 was only partially successful (see below) and therefore capable of further improvement.

### 7. Further Discussions on Sections with Peaky Distributions

The special merits of the sections with peaky distributions spring from the favourable manner in which the supersonic flow is able to develop to keep the shock weak and so to delay the onset of wave drag and shock-induced separation. This is clearly seen in Fig. 18 where the results for a triangular distribution are contrasted with those for a peaky distribution that was produced by extending the chord<sup>(24)</sup> of the basic section. The actual value of the peak suction is approximately the same for both aerofoils at low speeds (Fig. 18(a)) and the difference in the character of the distributions is most clearly seen in the shape of the suction loops. When  $M_0$  is increased to 0.7, Fig. 18(b), the triangular distribution develops a strong shock and a severe separation (Fig. 19), with local Mach number building up to a maximum at the shock. The peaky distribution on the other hand generates a strong expansion which is reflected from the sonic boundary to give a useful isentropic compression at the surface and a substantial reduction in shock strength to eliminate the separation. The part played by the peak is also clear from the changes that occur on the extended section when  $M_0$  is increased still further. As the peak drops (Fig. 18(b))

(due to a movement of the stagnation point) so the shock upstream Mach number and shock strength increase, with separation again developing (Fig. 19).

It is instructive to examine the effect of adding disturbances near the beginning of a given supersonic region. Consider first a single infinitesi-

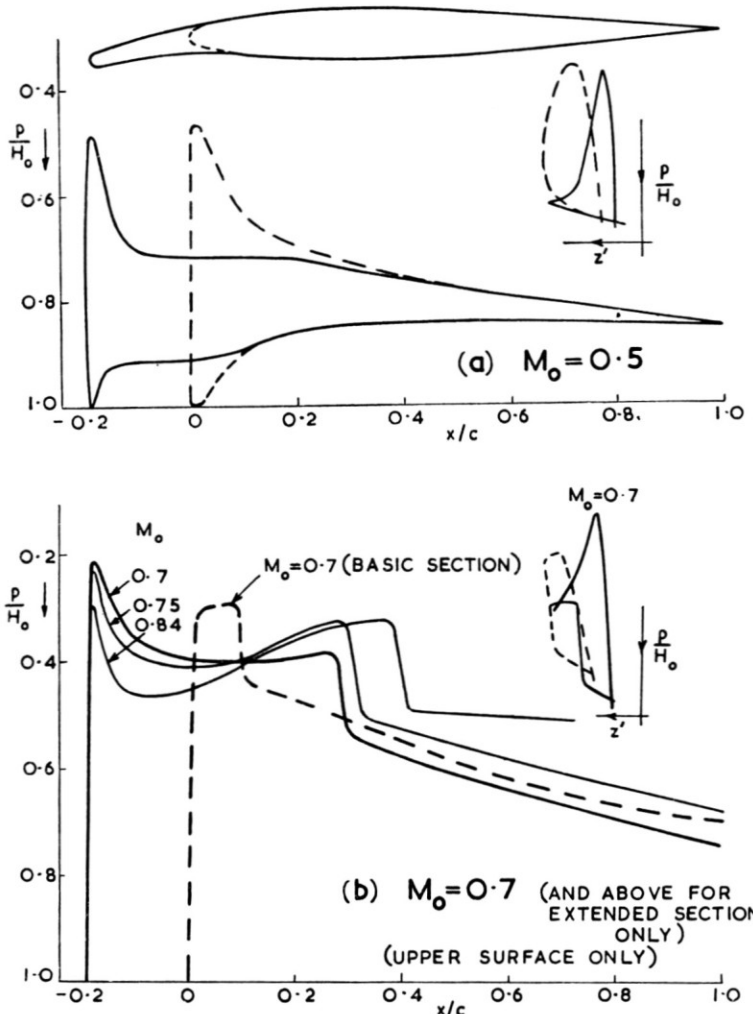


FIG. 18. Supersonic flow development from different leading-edge shapes ( $\alpha=7^\circ$ ).

mally small disturbance that can be represented by a Mach wave (Fig. 20(i)). This will be reflected with change of sign at the constant-pressure sonic boundary and again without change of sign when it returns to the surface, and so on. The net result at the surface is a "square wave" disturbance to the original distribution, with a change of sign at each reflection

at the surface. The addition of an expansion near the leading edge can thus simultaneously give extra suction there and reduce the strength of the shock at certain positions downstream. Consider next the addition

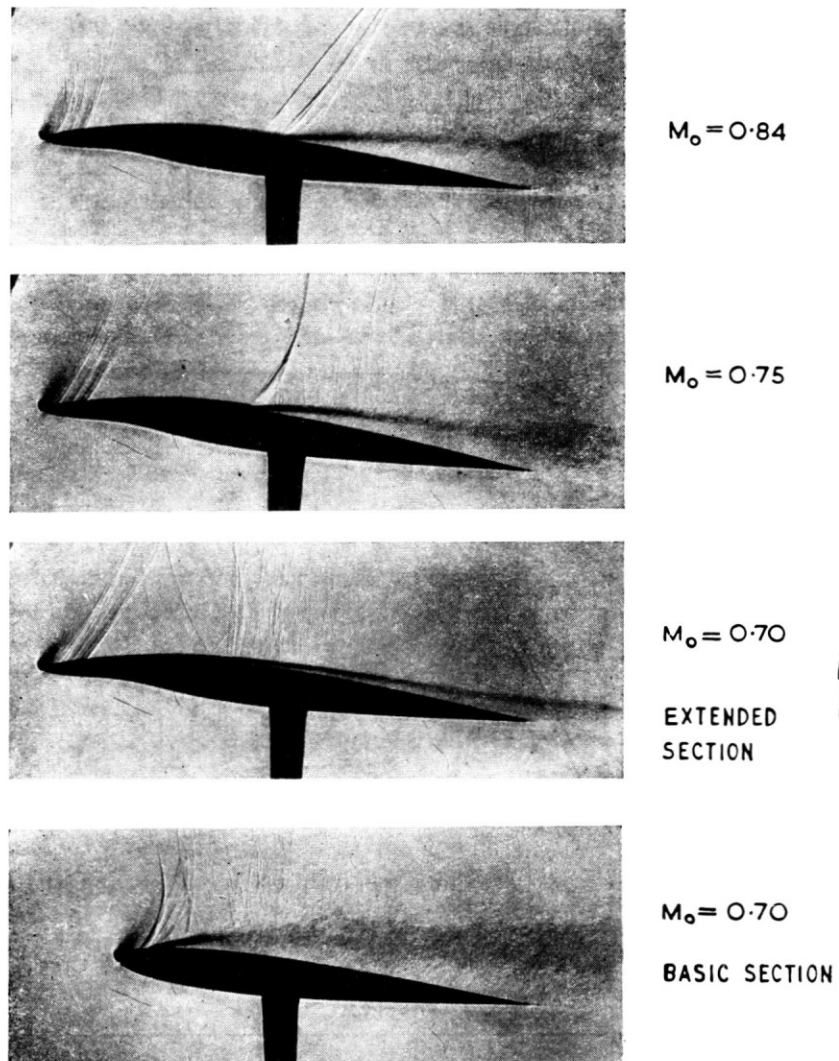


FIG. 19. Schlieren photographs for results of FIG. 18.

of a finite expansion as in Fig. 20(ii). The top diagram (*a*) shows just the correct degree of expansion with the maximum advantage in the desired chordwise region. If the expansion is too great (*b*) the reflected compressions cannot cancel the original disturbance within the chordwise region of interest. For too small an expansion (*c*) the advantage becomes too

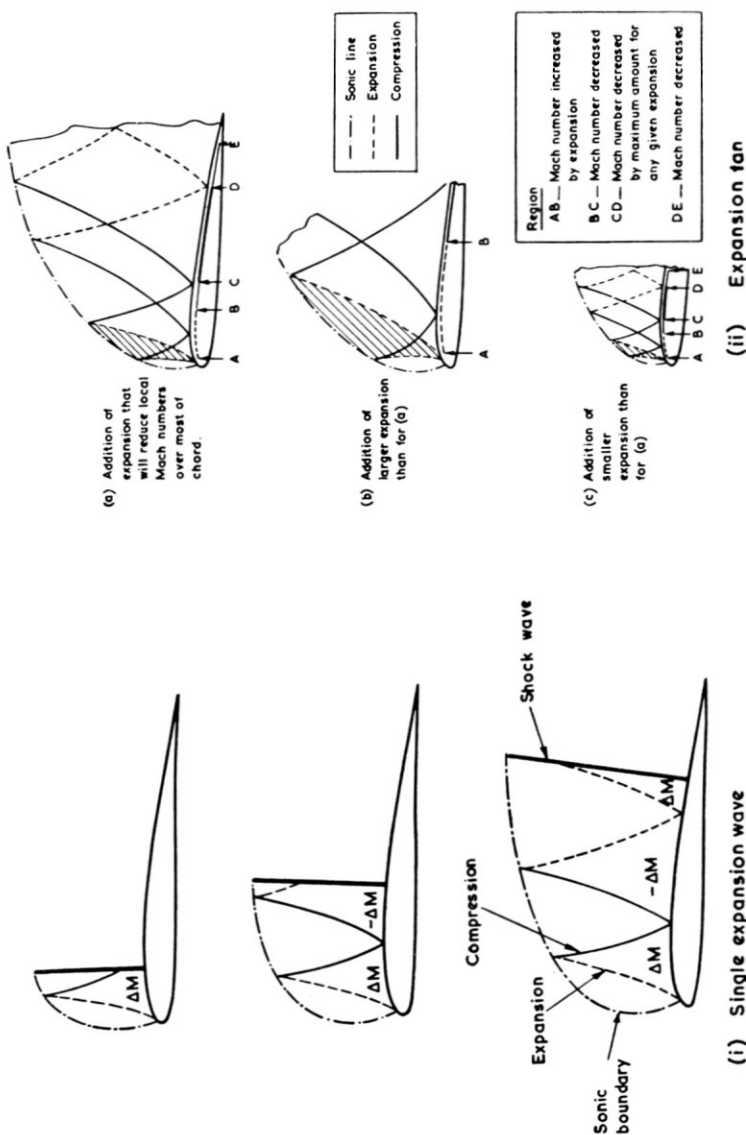


FIG. 20. The effect of adding disturbances to given flow.

small and too local to be worthwhile, and may turn into a definite disadvantage after a repeated reflection. Examples of all these situations are observed in practice—good results in some cases; too much expansion in others, particularly for very thin uncambered aerofoils at incidence where reduction of thickness has often proved a disadvantage; and too little expansion in yet others, as for example where too much camber or rounding of the leading edge has been applied to moderately thick sections with detriment at high speeds. The secret of design to exploit the favourable flow lies in achieving just the correct degree of expansion, but this has not proved amenable to theory so far, because the development of the supersonic flow does not conform to the pattern of Fig. 6 that is treated by the method of ref. 21. We shall return to this point later in Section 8.2.

### *8. Application of the Method of Characteristics*

8.1 *Connected points*—In feeling towards a solution to these flows, Sinnott and Stuart<sup>(25)</sup> have shown that the characteristics pattern in the locally supersonic region can be determined once the sonic point at the surface and the distribution of surface pressure in the supersonic flow downstream of this point are known. This offers a method of improving given section shapes once they have been tested—by introducing expansions at the correct upstream points, for example.

A very simple, but potentially extremely useful method for analysing known flows and for deriving an iterative empirical method of design arises from this approach. Thus, on a given characteristic,  $\Theta - \omega = \Theta_s$  or  $\Theta + \omega = \Theta_s$  according to which of the two families it belongs (Fig. 21), where  $\Theta$  is here the local flow direction,  $\Theta_s$  the flow direction at the sonic point of the characteristic and  $\omega$  the Prandtl-Meyer angle corresponding to the local Mach number of the flow. Now for a pair of characteristics connected via the sonic point as shown in Fig. 21,  $\Theta_1 - \omega_1 = \Theta_s = \Theta_2 + \omega_2$ . Conversely, if  $\Theta_1 - \omega_1 = \Theta_2 + \omega_2$  for any two points A, B at the surface, the characteristics from these will in general meet on the sonic line, and an infinitesimal disturbance introduced at A will return to the surface again at B, with change of sign.

Now  $\omega$  can be found at all points on the surface from the observed distribution of local Mach number, and since  $\Theta$  is also known at the surface, we can plot curves of  $\Theta + \omega$  and  $\Theta - \omega$  along the surface as in Fig. 21, and then select pairs of connected points simply by drawing horizontal intercepts, A' B''. We can thus find immediately where to modify the surface in order to reduce the shock strength in the desired downstream position. The danger of repeated reflections can also be spotted by drawing step intercepts such as A'B''B'C''.

Further analysis can be made on the basis of a few simple properties of the  $\theta - \omega$  and  $\theta + \omega$  curves, Fig. 22. Firstly, of course, the curve of surface slope variation,  $\theta$ , bisects the vertical intercept between them.\*

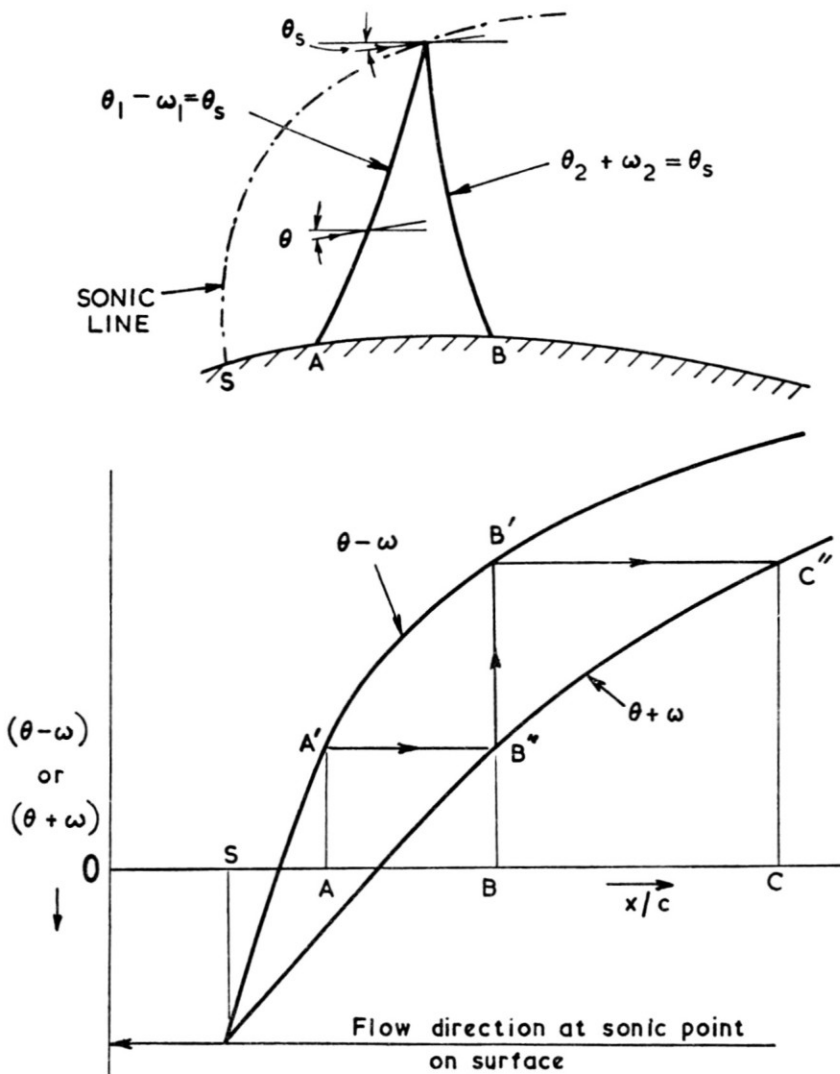


FIG. 21. Definition and selection of connected points.

The ordinate,  $XB''$ , Fig. 22(a), of the curve  $\theta + \omega$  gives the total compressive effect that has returned to the surface up to the point  $X(B)$ , and the

\* Since the position of the zero on the vertical scale has no particular merit in the present context, this fact is useful in deriving the characteristic curves locally from the  $\theta$  curve when the position of the sonic point on the surface is not known accurately.

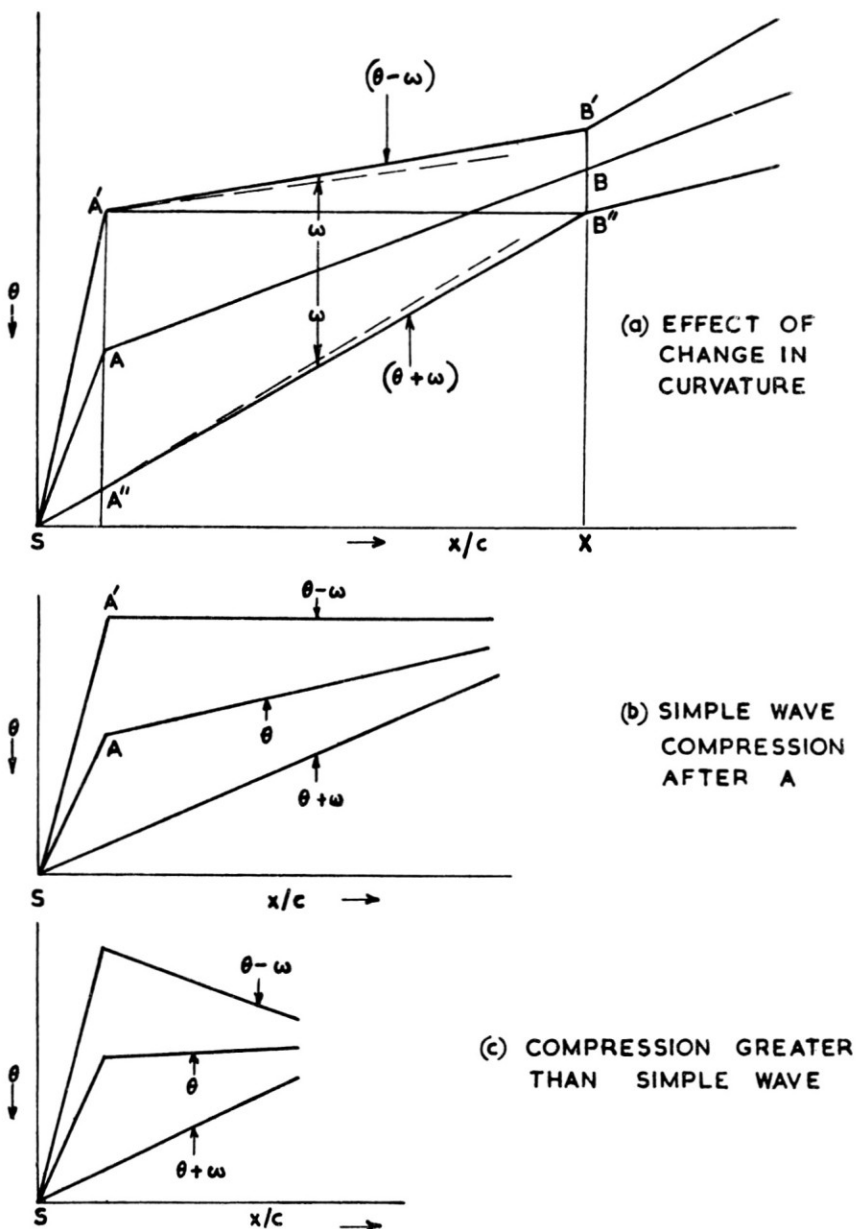


FIG. 22. Examples of connected-point analysis.

slope of the curve at any particular point gives the strength of the disturbance on the incoming family of characteristics at that point. Thus, the rate of change of  $\omega$  (hence of local Mach number) depends on the relative slopes of the  $\Theta$  and  $\Theta + \omega$  curves. In particular, a convergence of these

curves gives the compressions that are a feature of peaky sections. The simple sketches in Fig. 22 in fact show how the compression is created by using a high surface-curvature\* at the beginning of the supersonic region, and then decreasing it abruptly to a low one; for simplicity this reduction is assumed to be discontinuous at A. To the first order, the slope of  $\Theta + \omega$  is unaltered until the characteristic of the  $\Theta - \omega$  family (represented by A') returns to the surface (as B') at B, and so the required convergence is established.† B represents the downstream limit of the compressions reflected from the expansions generated in the region SA of high curvature. Beyond B, the slope of  $\Theta + \omega$  falls and  $\omega$  increases again.

Zero slope on the  $\Theta + \omega$  curve represents a simple wave on the  $\Theta - \omega$ , or outgoing, family, and, conversely, zero slope on the  $\Theta - \omega$  curve shows a simple wave on the  $\Theta + \omega$ , or incoming, family. For a convex surface, Fig. 22(b), the latter implies that for each point on the surface, the reflection of the compression on the incoming characteristic and the expansion generated by the surface are self cancelling, leaving just the compression on the incoming family. The compressions represented by Figs. 22(b) and (c) can occur isentropically, for short distances at least, but the full characteristics network would be needed to establish how far any particular one will proceed without the formation of shock waves.

**8.2 Peaky-section design**—Fig. 23 presents a connected point analysis of the results given previously in Figs. 18 and 19, and reveals that the favourable result for the extended section at  $M_0 = 0.7$  was established in the manner just described, except that the surface-curvature decrease from A is more gradual. The initial expansion is such that its last ray (on the characteristic A') is reflected to the surface (on B') immediately upstream of the shock at B, and is thus ideal in the sense that all the reflected compressions are used in weakening the shock. The compression is a simple wave at first, and could have reduced  $\omega$  to zero had the surface curvature not increased again where the extension blended into the basic section. It seems, in fact, that a change in the surface-slope distribution would be the only way of improving on this flow. Thus, for the given  $\Theta$  distribution, if  $\Theta - \omega$  were higher on the page at A',  $\Theta + \omega$  would be lower at B''. The downstream point connected to A' would thus be beyond the shock and the compression would not be used to the full advantage;  $\omega$  would also be greater at the shock. We should thus have the situation represented by the middle diagram of Fig. 20(ii). Conversely, if  $\Theta - \omega$

\* Or, more particularly, a high value of  $d\Theta/dx$ .

† A second order change will occur in practice, as indicated by the broken lines, because the change in strength of the disturbance on the outgoing characteristics between A and B will deflect the incoming characteristics that have originated from further upstream.

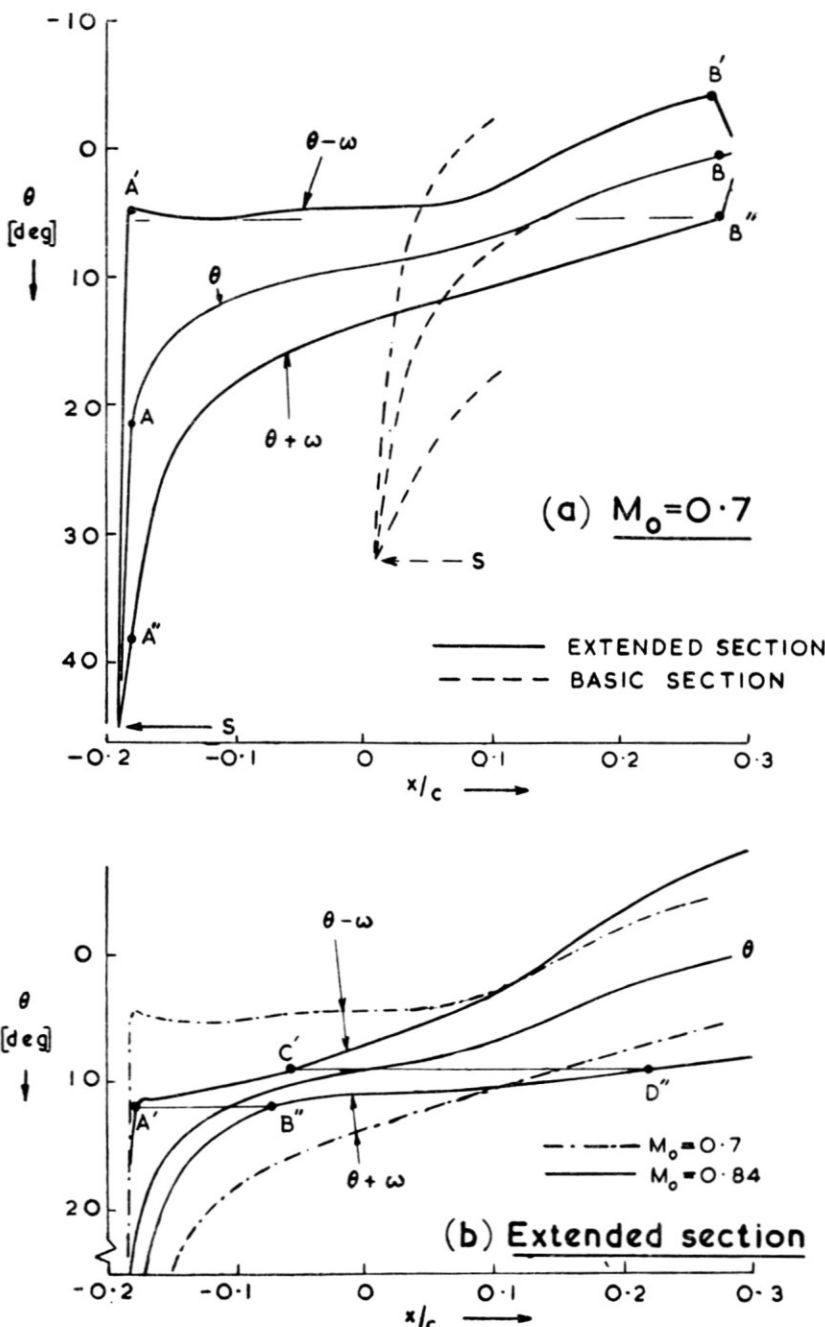


FIG. 23. Connected-point analysis for results of FIG. 18.

were lower at A', the beneficial effect of the initial expansion would be limited to a very small range of the chord (as in the lower diagram of Fig. 20(ii)). This explains immediately why the flow on the extended section (Figs. 18 and 19) deteriorated as  $M_0$  was increased from 0·7. Thus, for  $M_0 = 0\cdot84$  (Fig. 23(b)) the point B'' had moved very near to the leading edge.

The contrast between the full and broken lines in Fig. 23(a) illustrates the reason for the strong difference between the extended and basic sections. A vital feature of the full lines (and of all peaky sections) is that at the point at which the curvature starts to fall rapidly, the value of  $\omega$  and the slope of the  $\Theta + \omega$  curve are both high enough for the curve of  $\Theta + \omega$  to close towards, and if possible on to the curve of  $\Theta$  at the appropriate downstream point. For the broken lines, which are typical for sections on which the curvature decreases progressively from an early stage, the  $\Theta + \omega$  and  $\Theta$  curves are never convergent.

We can now enumerate features that are essential for the success of a peaky-section design. The first is the attainment of a certain peak value of  $\omega$ ,  $\omega$  (peak), in the rapid expansion from the stagnation point, combined with a fairly abrupt change from a high to a low surface curvature under the peak. Then,  $\omega$  (peak) and the distribution of surface slope ( $\Theta$ ) have to be matched in such a way that  $\Theta$  (peak) -  $\omega$  (peak) can equal  $\Theta$  (shock) +  $\omega$  (shock), with  $\omega$  (shock) having its desired low value, i.e. in such a way that characteristic A' is connected to characteristic B'' with the vertical distance BB'' small.\* In designing for this it might be possible to derive  $\omega$  (peak) by analogy with the subsonic pressure distribution because the expansion from stagnation point to peak seems to follow the subsonic pattern, for the initial stages of the supersonic flow development at least. The attainment of these individual features need not by itself ensure an isentropic compression from peak to main shock, and it might be necessary to iterate from a known isentropic flow for which the full characteristics network can be constructed.

At the start of the present series of experiments a small leading-edge radius was thought to be essential for establishing the desired supersonic flow. That this is not so can be seen from the comparison in Fig. 24 for a 4:1 increase in leading-edge radius for which the extra thickness was accommodated on the lower surface to leave the upper-surface pressures and slopes almost unaltered. This change produced almost identical results and so encouraged the view that the peaky section need not be in-

\* In designing in practice for a range of  $M_0$  and  $a$ , i.e. for a range of shock and stagnation positions, it would be necessary to accept a range of reasonably low values of  $\omega$ .

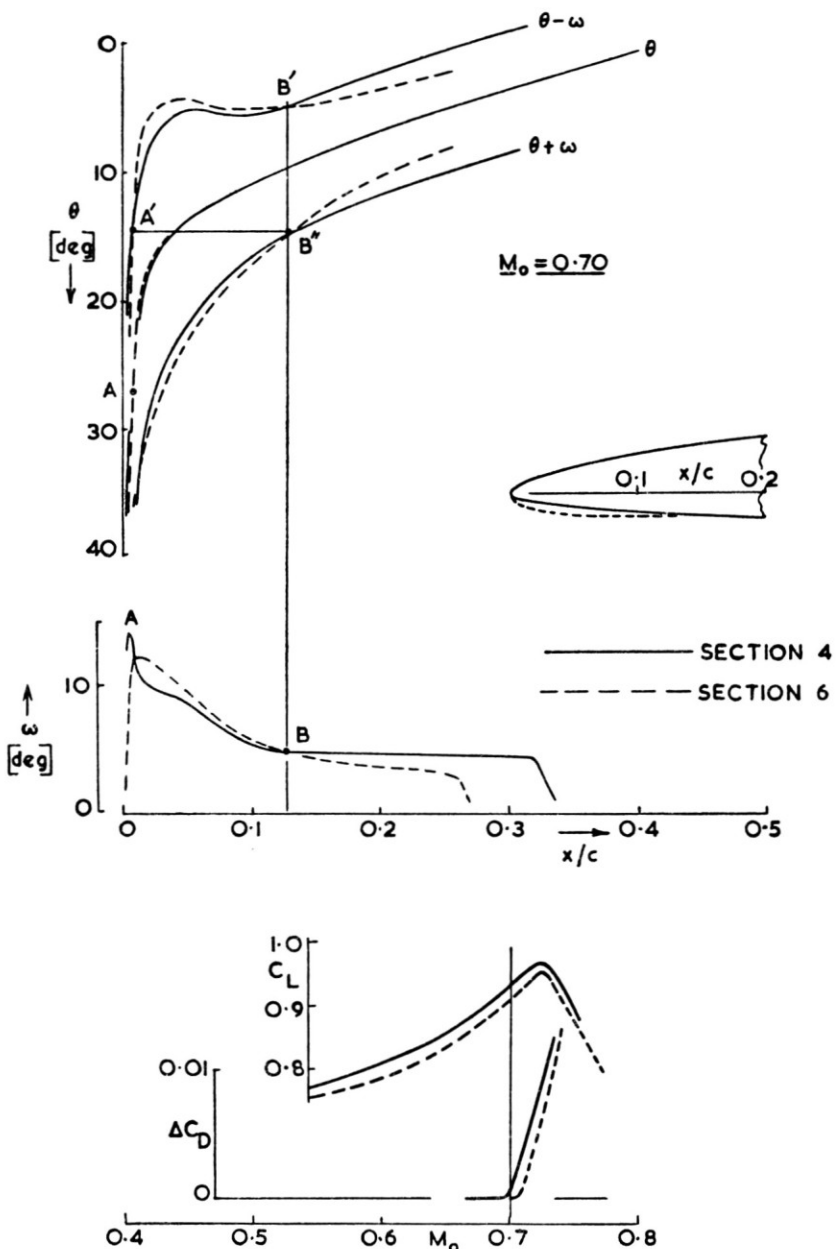


FIG. 24. Change of leading-edge shape on peaky section.

compatible with good airfield performance. The slight differences in favour of the modified section 6, which at  $M_0 = 0.7$  are apparent from the reduction in  $\omega$  at points beyond B, and from the associated convergence between  $\theta$  and  $\theta + \omega$ , can be traced from B to a point A very near to the

leading edge where a small irregular change in curvature for section 4 (not discernible in the scales used here) was incidentally smoothed out in the re-design. This suggests that very careful shaping is required for the immediate leading-edge region.

### 9. *The Choice of Conventional Section*

9.1 *Two-dimensional design*—The present work has confirmed that this choice can be made, and the design assessed and developed, on the basis of surface pressure and slope distributions on the upper-surface. With these features of the design fixed, the thickness and camber, and their distributions, can be derived to give the required structural and lifting characteristics.

If the cruise flow has to be entirely subsonic in type, or shock free, the roof-top upper-surface pressure distribution, which ensures that the additive super-velocities due to thickness and lift do not exceed a certain maximum, is obviously the best. The limit to the rearward extension of the plateau (defined by  $X_1$  in Fig. 4) is imposed by reduced margins before the onset of shock-induced separation (see Fig. 11) and the increased severity of the boundary-layer growth under the adverse gradient towards the rear of the section that occurs even in the absence of shock waves.\* For a design that has to be really conservative in these respects the limit can be quite small, of the order of 30% chord, but is dependent on the degree of sweepback (see below). The incorporation of a boundary-layer control device at the design stage in order to exploit the potentialities of the roof-top section thus appears as an attractive proposition.<sup>(5)</sup>

The peaky section, which in effect uses a supersonic peak suction generated by the lift super-velocity to produce a favourable cancelling effect on shock strength, offers a significant gain over the roof-top section in drag rise and the best chance of reconciling good drag-rise characteristics with adequate margins before shock-induced separation. The boundary-layer growth at the rear can be made less severe, in spite of the peak suction, and the possibility of using a comparatively large leading-edge radius also offers promise of a better reconciliation with good airfield performance. Recent results have shown that the gains are real, but the design remains empirical and possibly critical to small changes of shape very near to the leading edge.

The analysis of the strong influence that surface-slope distribution exerts on the development of the local supersonic flow has demonstrated

\* Results like those in Fig. 5 indicate that this boundary-layer growth and its effects on lift and drag are again dependent on the upper-surface pressure distribution rather than on  $C_L$  or thickness. The boundary-layer growth can be calculated for two-dimensional flow(26).

that, even if the favourable effects of the peaky distribution are not exploited at the cruise, the surface-slope distribution should be chosen to encourage its development with increase in  $C_L$  above the cruise and, conversely, to avoid the type of flow shown for the basic section in Figs. 18 and 19. This flow is characteristic for sections with gradually reducing curvature; it can lead to really serious limitations in the margins of usable  $C_L$  and also inhibit the stretching so often sought for in later developments of particular designs.

*9.2 Application to swept wings*—The validity of the approach has already been proved for wings of moderate degrees of sweep, and will soon be put to the test for finite wings of higher sweep like the one described by Lock and Rogers<sup>(2)</sup> for which root and tip effects are successfully eliminated. The major remaining uncertainties relate to viscous effects. For example, certain model tests have suggested that the boundary-layer growth to the rear of sections with far back roof tops, and the associated rear separations, can have disastrous effects for high degrees of sweep ( $55^\circ$ – $60^\circ$ , say). The degree of severity to be expected at full scale is not yet known, however. For shock-induced separations, on the other hand, there is reason to believe<sup>(27)</sup> that the effect of sweep is more favourable than would be predicted on the simple yawed-wing analogy.

The correct design for isentropic compression from a supersonic suction peak may become increasingly critical on highly swept leading edges, although the results described by Lock and Rogers<sup>(2)</sup> indicate that a similar compression downstream from the ridge line of a diamond section was unaltered by sweep.

A further uncertainty arises for finite wings, on which the design to achieve a particular subsonic-type pressure distribution uniformly across the span involves wing warp and hence differences in wing geometry that could lead to differences in the supersonic flow developed locally on different parts of the span.

The work just described does not, of course, take into account the possible advantages to be gained from the deliberate use of spanwise variations in section shape to exploit favourable three-dimension flow characteristic such as increased isobar sweep<sup>(28)</sup>.

#### 10. Novel Approaches

Since no conventional design can be found that is outstandingly promising in all directions, and since further aerodynamic gains are sought continuously, one is led to consider other, more novel possibilities.

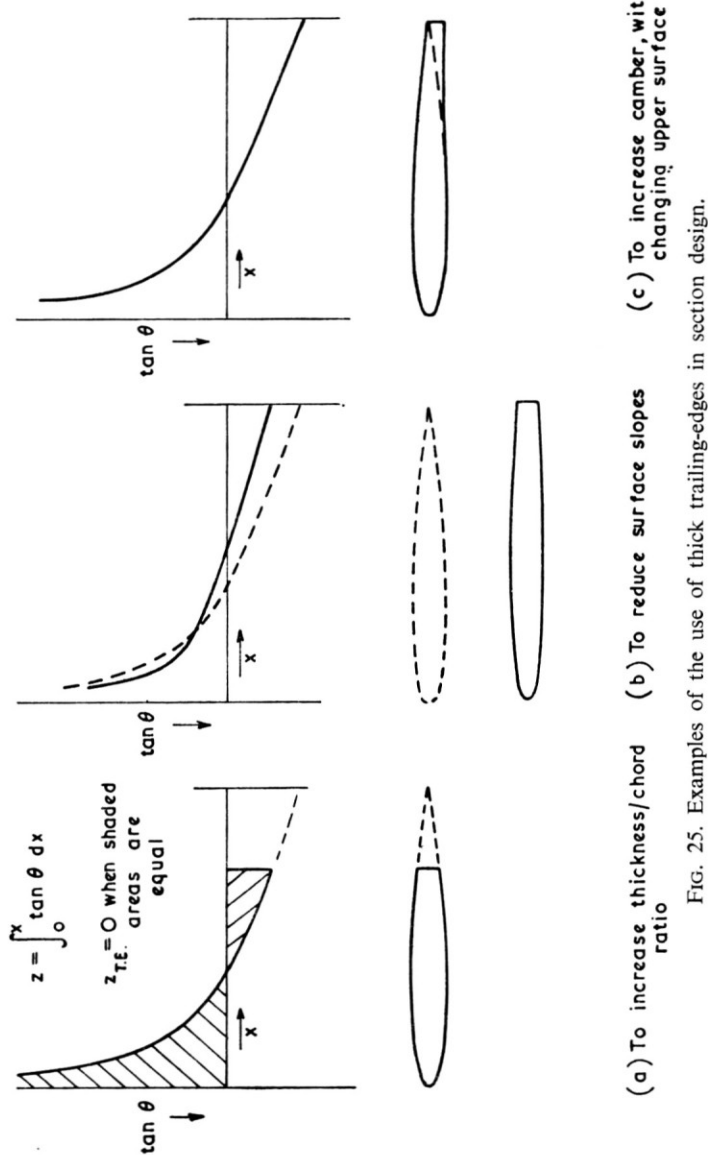
*10.1 Laminarization*—Since this would eliminate the adverse effects of turbulent boundary-layer growth at the rear of roof-top sections and provide boundary-layer control to prevent shock-induced separation, it

would remove the restrictions to extending the plateau. The advantage of the resulting higher drag-rise Mach number (or its equivalent in increased thickness, increased lift coefficient or reduced sweepback) can thus be written on the credit side of the complicated laminarization balance sheet.

10.2 *Thick trailing edges*—The work on section design has pointed to the great importance of the distribution of surface slope on the upper surface. For sharp trailing edges, the geometrical requirement that the curve of  $dz/dx$  (Fig. 25) should generate equal areas above and below the axis imposes severe limitations on the choice of slope distribution. The thick trailing edge can be considered as a device for relaxing this requirement and hence for allowing: an increase in thickness/chord ratio without any increase in upper-surface slopes (Fig. 25(a)); reduced surface slopes for a given thickness/chord ratio (Fig. 25(b)); or increased camber without the usual increase in upper-surface slope (Fig. 25(c)). It can further be argued that to the advantages thus to be gained on drag rise, and on the occurrence of separation at the shock waves, can be added an increased delay in the onset of the effects of the separation arising from the manner in which the thick trailing edge shields the lower surface from the influence of the separation on the upper surface<sup>(22)</sup>. The base drag could, of course, be a strong disadvantage.

Some research has already been done at the NPL to study the first two of the three applications enumerated, using fairly large degrees of thickening. This has confirmed that, for attached flow, the pressure distribution on the blunt section can be derived from that on the corresponding part of the same section extended smoothly to a sharp trailing edge and held at the same local incidence to the airstream, and also that the reaction to separated flow is less severe. The need now would seem to be to obtain systematic data on the base-drag penalty for various degrees of thickening, from small values upwards, and on the possibilities of base-drag reduction, so that design assessments can be made. Also, the third possible application (i.e. to increase camber) still has to be investigated.

In designing a section to study the second application (i.e. reduced surface-slopes for a given thickness/chord ratio), we started with the front part of an extremely thin section (Fig. 26) which we expected to be poor under lifting conditions. We therefore incorporated a drooped extension to reduce the expansion to a better level for a peaky section and so to improve the performance at worthwhile lift coefficients. The success of this has been shown in recent tests by Holder<sup>(23)</sup> (Fig. 26). For the particular incidence illustrated, the isentropic compression from the leading-edge peak was just right to give very small wave drag at  $M_0 = 0.9$  and



$C_L = 0.54$  (and this for an unswept wing). From  $M_0 = 0.6$  onwards, the supersonic flow development was such that it gave the necessary super-velocities to allow the lift-coefficient to continue to increase nearly

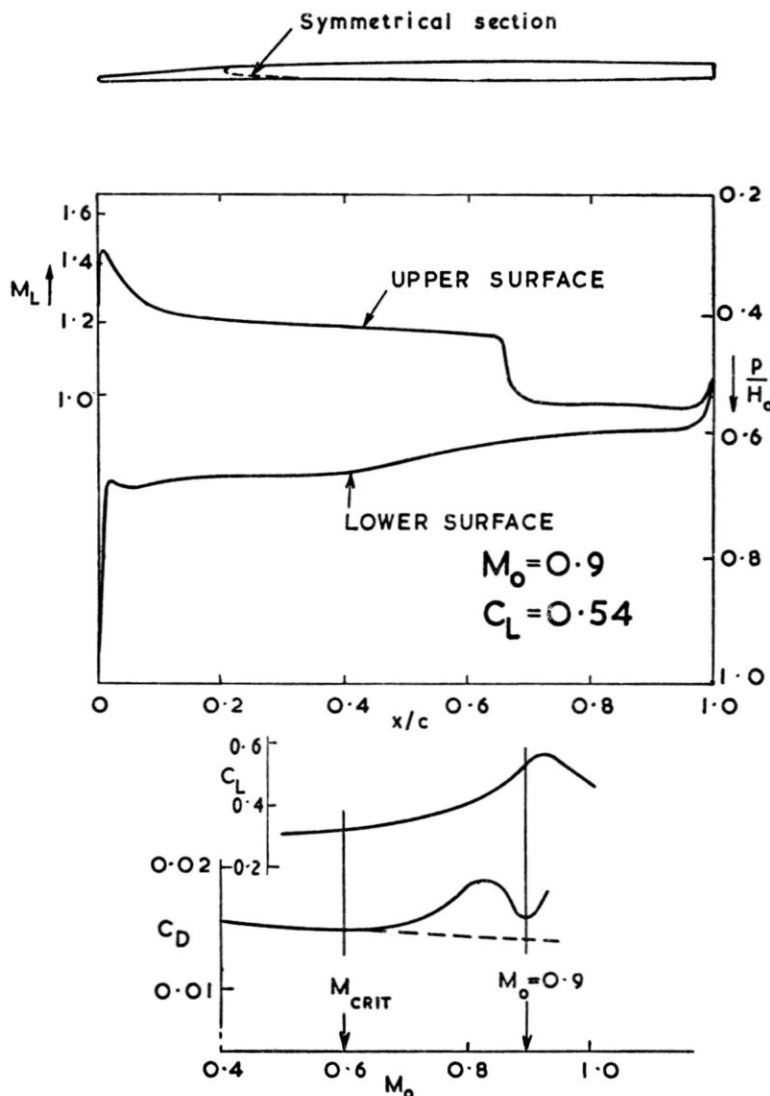


FIG. 26. Results for 3.2% thick section with thick trailing-edge at  $\alpha=3^\circ$ .

two-fold, but at the same time could so successfully reduce shock strength as to keep the increase in wave drag to a very low level. However, in this particular case, the highly favourable result was obtained for a very small range of  $M_0$  and  $C_L$  only.

Whitcomb<sup>(30)</sup> has demonstrated that the advantages of thick trailing-edge section can be obtained successfully on a swept wing on which discrete bodies are added to give an equivalent section shape that is thinner and less highly curved than the actual one (Fig. 27) and for which the bodies are used as engine nacelles so that the finite trailing-edge thickness is cunningly replaced by the jets. The bodies have the additional advantage of providing boundary-layer fences to eliminate the effects of rear separations<sup>(30)</sup>.

**Section through nacelle**

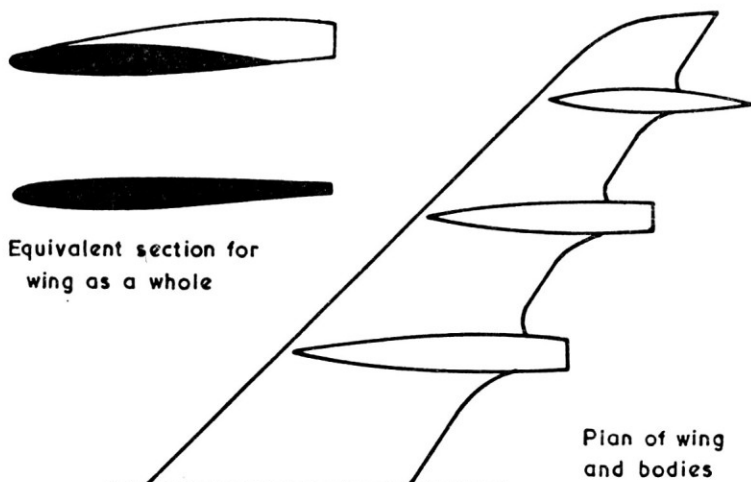


FIG. 27. Method for incorporating equivalent sections with blunt trailing edges (see Whitcomb<sup>(22)</sup>).

10.3 *The jet or Thwaites-flap*—The chordwise load distribution for weak jet flaps<sup>(10)</sup> or small trailing-edge spoilers<sup>(31)</sup> is approximately constant but carries peaks at the leading and trailing edges. One is therefore led to speculate that some such device might embrace the potential advantages of a roof-top section with plateau extending towards the trailing edge, those of a peaky section, and those of a section with thick trailing edge (but somewhat rounded so that the boundary layer could be persuaded, by boundary-layer control, to follow the base to a rear stagnation point).

### 11. Concluding Remarks

In conclusion, the implications of the various observed results can conveniently be compared with one another, and with theoretical prediction for some straightforward example, on the framework provided

by Bagley's<sup>(6)</sup> prediction of the combinations of streamwise thickness, actual  $C_L$ , and sweepback that can be used for a shock-free flow at  $M_0 = 1.2$ , assuming an upper surface roof-top velocity distribution to 30% chord. This is done in Fig. 28, where the lines show the theoretical results for specified sweep angles. The symbols are derived from selected observations on two-dimensional aerofoils by the standard transformation

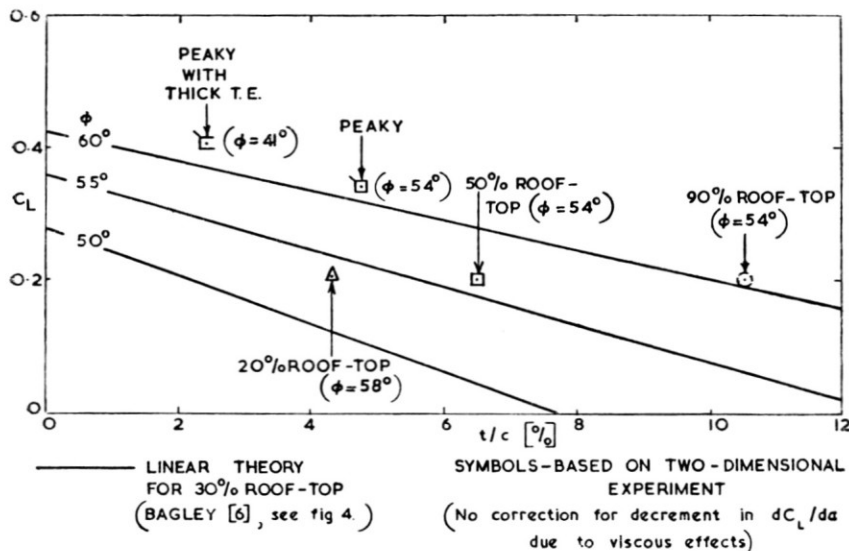


FIG. 28. Estimated design conditions to give onset of wing wave-drag at  $M_1 = 1.2$ .

(Eqns (1) to (3). The differences between the experimental values for sweepback (figures in brackets) and the interpolated theoretical ones to give the same  $t/c$  and  $C_L$  then provide a measure of the success of the designs (Table 2). The relative gains could alternatively be derived in

TABLE 2  
Analysis of results in Fig. 28

| Type of section                | Advantage over Bagley's prediction (sweep angle) | Derivation                   |
|--------------------------------|--|------------------------------|
| 20% roof-top                   | -4°  | Section 2                    |
| 50% roof-top                   | +2°  | Sections 1 and 11            |
| Peaky                          | +7°  | Sections 4 and 6             |
| 90% roof-top                   | +7°  | Estimated from 11 and Bagley |
| Peaky with thick trailing edge | +21°   | Section of Fig. 26           |

terms of thickness or  $C_L$ . The absolute comparison with theory will be influenced by the viscous decrement on  $dC_L/d\alpha$  in the experiments, but the relative merits of the experimental results should be represented correctly.

This comparison provides an excellent summary of the discussions in sections 5 to 10 of the paper regarding the onset of shock-wave drag. In order to use the large potential advantage of the thick trailing-edge section, some efficient means for reducing base drag is likely to be required. Some form of boundary-layer control may well be needed with the 50% roof-top, and the result for the 90% roof-top is, of course, a speculation that would depend on the success of laminarization or of a Thwaites flap type of control on circulation. The advantages of the peaky section are left as probably the most readily realizable, but the design remains empirical. This is, however, a field in which resort to empiricism has frequently been necessary and fruitful.

## 12. Acknowledgements

The author would again formally but sincerely acknowledge the help that this work has received from the Royal Aircraft Establishment and the British aircraft industry. He is also grateful to Mr. J. Osborne and Miss I. J. Cox for help in the preparation of this paper.

The work has formed part of the research programme of the National Physical Laboratory and is presented by permission of the Director of the Laboratory.

## NOTATION

|           |   |
|-----------|---|
| $M$       | Mach number   |
| $p$       | static pressure   |
| $H$       | stagnation pressure   |
| Suffixes  |   |
| 0         | value in the undisturbed stream                                 |
| 1         | value immediately upstream of shock wave                        |
| 2         | value immediately downstream of shock wave                      |
| $M_L$     | local Mach number on the surface                                |
| $M_D$     | drag-rise Mach number   |
| $M_0^*$   | free-stream Mach number for which $M_L = 1.0$ at aerofoil crest |
| $L, D$    | lift, drag  |
| $C_{L,D}$ | lift-, drag-coefficients  |
| $C_p$     | pressure-coefficient  |
| $\phi$    | angle of sweepback  |
| $\omega$  | Prandtl-Meyer angle for the local flow ( $M_L > 1.0$ )          |

|                 |  |
|-----------------|--|
| $\theta$        | surface slope (and local flow direction)     |
| $\delta_{T.E.}$ | trailing-edge flow deflection (see Fig. 7)   |
| $\chi$          | parameter of leading-edge shape (see Fig. 7) |
| $\alpha$        | angle of incidence                           |
| $c$             | aerofoil chord                               |
| $t$             | aerofoil thickness                           |
| $x, z$          | aerofoil co-ordinates                        |
| $z'$            | see Fig. 15                                  |
| $\chi_1$        | see Fig. 4                                   |

## REFERENCES

1. KÜCHEMANN, D., Aircraft shapes and their aerodynamics for flight at supersonic speeds. Paper for I.C.A.S. Conference, Zürich, (1960)
2. LOCK, R. C. and ROGERS, E. W. E., Aerodynamic design of swept wings and bodies for transonic speeds. Paper for I.C.A.S. Conference, Zürich, (1960)
3. PEARCEY, H. H., Shock-induced separation and its prevention by design and boundary layer control. Contribution to *Boundary Layer and Flow Control* (ed. G. V. LACHMANN) Pergamon Press (1960)
4. HAINES, A. B., HOLDER, D. W. and PEARCEY, H. H., Scale effects at high subsonic and transonic speeds, and methods for fixing boundary-layer transition in model experiments. ARC R and M 3012 (1954)
5. PEARCEY, H. H. and STUART, C. M., Methods of boundary-layer control for postponing and alleviating buffeting and other effects of shock-induced separation. IAS S.M.F. Fund Paper FF-22 June, 1959
6. BAGLEY, J. A., Unpublished RAE Report
7. JENKINS P. D., and PEARCEY, H. H., Unpublished NPL Report
8. WEBER, J., The calculation of the pressure distribution over the surface of two dimensional and swept wings with symmetrical aerofoil sections. ARC R and M 2918 (1956); see also The calculation of the pressure distribution on the surface of thick cambered wings and the design of wings with given pressure distribution. ARC 17, 927 (1955)
9. TANNER, L. H., Curves suitable for families of aerofoils with variable maximum thickness position, nose radius, camber and nose droop. ARC C.P. 358 (1957)
10. Ed. THWAITES, B., *Incompressible Aerodynamics*. Oxford Univ. Press (1960)
11. PEARCEY, H. H., SINNOTT, C. S. and OSBORNE, J., Some effects of wind tunnel and interference observed in tests on two-dimensional aerofoils at high subsonic and transonic speeds. NPL/Aero/373 (1959)
12. OSBORNE, J. and SINNOTT, C. S., The use of simple compressibility formulae in transonic flow ARC 21, 860 (1960)
13. WOODS, L. C., The application of the polygon method to the calculation of the compressible subsonic flow round two-dimensional profiles. ARC C.P. 115 (1952)
14. SINNOTT, C. S., On the flow of a sonic stream past an airfoil surface. *J. Ae./Sp. Sci.*, March, 1959
15. HOLDER, D. W., Note on the flow near the tail of a two-dimensional aerofoil moving at a free-stream Mach number close to unity. ARC C.P. 188 (1954)
16. SINNOTT, C. S., Estimation of the transonic characteristics of aerofoils. NPL/Aero/385 (1959). (To be published in *J. Ae./Sp. Sci.*)

17. RANDALL, D. G., Transonic flow over two-dimensional round-nosed aerofoils ARC 20, 677 (1958)
18. ACKERET, J., FELDMANN, F. and ROTT, N., Unberuchungen an Verdichtungsstössen und Grenzschichten in schnell bewegten Gassen. ETH, Zürich Report No. 10 (1946)
19. EMMONS, H. W., The theoretical flow of a frictionless, adiabatic, perfect gas inside of a two-dimensional hyperbolic nozzle. NACA TN 1003 (1946)
20. GADD, G. E. and HOLDER, D. W., The behaviour of supersonic boundary layers in the presence of shock waves. Proceedings of the 7th Anglo-American Aeronautical Conference, New York (1959) (IAS Paper No. 59-138)
21. SINNOTT, C. S. and OSBORNE, J., Review and extension of transonic aerofoil theory ARC R and M. 3156 (1958)
22. PEARCEY, H. H., A method for the prediction of the onset of buffeting and other separation effect from wind tunnel tests on rigid models. ARC 20,631 (1958) AGARD Rep. No. 223
23. NITZBERG, G. E. and CRANDALL, S., A study of the application of aerofoil section data to the estimation of the high-subsonic-speed characteristics of swept wings. NACA RM A55C23. (1955)
24. FARREN, Sir WILLIAM., The Aerodynamic Art. 44th Wilbur Wright Lecture (1956) *J. Roy. Aero. Soc.* July 1956; K. NEWBY Unpublished RAE report (1955)
25. SINNOTT, C. S. and STUART, C. M., An analysis of the supersonic region in a high subsonic flow past an aerofoil surface. ARC 21, 715 (1960)
26. SPENCE, D. A., Prediction of the characteristics of two-dimensional aerofoils. *J. Aero. Sci.*, Vol. 21, No. 9, (1954)
27. ROGERS, E. W. E. and HALL, I. M., An introduction to the flow about plane swept-back wings at transonic speeds *J. Roy. Aero. Soc.* Aug. 1960 NPL/Aero/394 (1959)
28. HAINES, A. B., Wing section design for swept-back wings at transonic speeds. *J. Roy. Aero. Soc.* (1957)
29. HOLDER, D. W., Unpublished NPL work
30. WHITCOMB, R. T. and HEATH, A. R., Several methods for reducing the drag of transport configurations at high subsonic speeds. NASA Memo 2-25-59L (1959)
31. WOODS, L. C., Theory of aerofoil spoilers. ARC R and M 2969 (1953)

## DISCUSSION

A. B. HAINES: One of the main conclusions from Mr. Pearcey's paper is that he is recommending pressure distribution under cruising conditions which will tend to have a severe adverse pressure gradient concentrated over the rear part of the section. This is true of both the extended roof-top and the "peaky" types of section. In the written version of this paper, Mr. Pearcey mentions that certain model tests have suggested that the boundary-layer growth to the rear of such sections and the associated rear separations can have disastrous effects for high angles of sweep such as 55° or 60°. Some of these results have been obtained in the A.R.A. transonic tunnel and some comment by myself is therefore perhaps appropriate. The point I wish to emphasize is that these effects can be important under cruising and indeed under most conditions of flight. It is not merely a question, as so often in the past, of obtaining an adequate margin between the drag-rise or cruise condition and the boundary beyond which shock-induced separa-

tion occurs. If no measures are taken to control these boundary-layer effects, the drag-due-to-lift factors might be in the region of 1.5 to 2.0 rather than the values near 1.0 hoped for by Dr. Küchemann in his paper. To say no more would however present too gloomy a picture. Further results have shown that these effects can be drastically reduced by quite simple practical boundary-layer devices such as vortex generators. I could quote an example in which the addition of a set of vortex generators reduced  $K$  to near 1.0. Also, they improved the value of  $C_L$  beyond which the trailing-edge pressure diverged from about  $C_L = 0.15$  to about  $C_L = 0.45$  for a wing designed for  $C_L = 0.17$  (using section 11 in Mr. Pearcey's paper). What made this result even more impressive was that it was obtained with the first design of generators tried. It was not the result of a long series of tests to find the optimum design of generators. If there are objections on aesthetic grounds to the use of vortex generators, more refined methods of boundary layer control could be suggested to do the job even more efficiently. It should however be realized that it will probably be necessary to use such devices in the cruise and indeed under most flight conditions.

H. H. PEARCEY: I am very grateful to Mr. Haines for raising this very important point, namely that some boundary layer control may be needed even at the cruise for roof top sections with plateaus back to say 50% chord when used with high sweep backs (of the order of 50° and above), in order to prevent undue boundary layer drift and hence displacement effect and pressure drag. I am also pleased that he made it clear that this boundary-layer control need not be anything very complicated or difficult to engineer. I would, however, add one point to what he has said, namely that the strong boundary-layer effects to which he referred may be less severe at full-scale Reynolds number. (In this respect, they differ from the shock-induced separation effects which, if anything, become more severe at full scale.) It is important to obtain information on this point by testing at even higher Reynolds numbers than Mr. Haines can obtain in his wind tunnel.

The second point relates to the use of vortex generators. These are usually now accepted, even in the best circles. They in fact achieve what can be considered an advanced form of boundary-layer control by forced mixing, and can be designed on a scientific basis. The reason why Mr. Haines obtained good results with the first design of generators tried was in fact that this design conformed to a well-proved type.

R. M. COX: I would like to offer a warning to Mr. Pearcey on a point that I suspect he has already appreciated, namely that in his derivation of connected points the addition of a disturbance near the forward end of the local supersonic region will influence the characteristics downstream and so tend to invalidate further analysis on the basis of the undisturbed pressure distribution.

H. H. PEARCEY: Thank you for drawing attention to this important point. I should have said of course that the downstream connected point can be found only to the first order when the disturbance is added to the original flow unless one does a much more complicated characteristics analysis. However, the errors are quite small if the disturbance is not too large. This has been checked in a characteristics analysis of a complete local supersonic region.

W. F. HILTON: Mr. Pearcey has described how we should exploit the reflection of an expansion wave at the sonic line as a compression, and then reflect this compression from the wing as a compression. This reduces the losses in the normal shock. Can he suggest a method by which the increase of height of the sonic line above the wing can keep pace with the rearward movement of the shock-wave as Mach number is increased? In this way a wider range of cruise Mach numbers would be achieved.

H. H. PEARCEY: Dr. Hilton has, as usual, raised a very pertinent point. The height of the sonic line near the shock wave does in fact tend to increase naturally as the Mach number is increased but the height near the leading-edge tends to decrease. At present I am unable to suggest any means of countering this latter trend which certainly does tend to limit the range of cruise Mach numbers that can be achieved with the ideal type of reflection from the sonic boundary.